

Seismic Vulnerability and Risk Assessment of Historic Masonry Buildings

Romeu Vicente, Dina D' Ayala, Tiago Miguel Ferreira,
Humberto Varum, Aníbal Costa, J. A. R. Mendes da Silva
and Sergio Lagomarsino

Abstract Seismic risk evaluation of built-up areas involves analysis of the level of earthquake hazard of the region, building vulnerability and exposure. Within this approach that defines seismic risk, building vulnerability assessment assumes great importance, not only because of the obvious physical consequences in the eventual occurrence of a seismic event, but also because it is the one of the few potential aspects in which engineering research can intervene. In fact, rigorous vulnerability assessment of existing buildings and the implementation of appropriate retrofitting solutions can help to reduce the levels of physical damage, loss of life and the economic impact of future seismic events. Vulnerability studies of urban centres

R. Vicente (✉) · T. M. Ferreira · H. Varum · A. Costa
Civil Engineering Department, Aveiro University, 3810-193 Aveiro, Portugal
e-mail: romvic@ua.pt

T. M. Ferreira
e-mail: tmferreira@ua.pt

H. Varum
e-mail: hvarum@ua.pt

A. Costa
e-mail: agc@ua.pt

D. D' Ayala
Civil Environmental and Geomatic Engineering, University College London,
WC1E 6BT, London, UK
e-mail: d.d'ayala@ucl.ac.uk

S. Lagomarsino
Department of Structural and Geotechnical Engineering,
University of Genova, 16145 Genova, Italy
e-mail: sergio.lagomarsino@unige.it

J. A. R. M. da Silva
Civil Engineering Department, Coimbra University, 3030-788 Coimbra, Portugal
e-mail: raimundo@dec.uc.pt

should be developed with the aim of identifying building fragilities and reducing seismic risk. As part of the rehabilitation of the historic city centre of Coimbra, a complete identification and inspection survey of old masonry buildings has been carried out. The main purpose of this research is to discuss vulnerability assessment methodologies, particularly those of the first level, through the proposal and development of a method previously used to determine the level of vulnerability, in the assessment of physical damage and its relationship with seismic intensity.

Keywords Vulnerability • Risk • Masonry • Fragility curves • Damage scenarios

1 Vulnerability Assessment and Risk Evaluation

The assessment of the vulnerability of the building stock of an urban centre is an essential prerequisite to its seismic risk assessment. The other two ingredients are the expected hazard over given return periods and the distribution and values of the assets constituting the building stock. All three elements of the seismic risk assessment are affected by uncertainties of aleatory nature, related to the spatial variability of the parameters involved in the assessment, and epistemic, related to the limited capacity of the models used to capture all aspects of the seismic behaviour of buildings and of describing them in simple terms, suitable for this type of analysis. Hence it should always be kept in mind that the computation of a risk level is highly probabilistic, and that to accurately represent the risk the expected values should always be accompanied by a measure of the associated dispersion. A very preliminary estimate of the seismic capacity of the local building stock can be obtained by consulting the requirement included in the seismic standards and code of practices in force at the time of construction of such buildings. This information together with a temporal and spatial record of the growth of the urban centre can provide a first definition of classes of buildings assumed to have different capacity class by class. This information can be obtained by looking at past and present cadastral maps with ages of buildings and knowing the historical development and enforcement of codes at the site. In general however for a correct assessment of the seismic risk a more detailed inventory and classification should be considered, the extent of which is a function of the economic and technical resources available and of the extent of the area under investigation and the diversity within the building stock.

In the case of historic masonry buildings constituting the core of city centres data on their structural layout and lateral capacity cannot generally be obtained from seismic standard, as this do not include these buildings typologies. However in the last twenty years extensive historical studies on the development of so-called non engineered structural typologies and documentation of the associated local construction techniques have been produced in many region of Europe exposed to significant earthquake hazard. These studies tend to provide construction details and qualitative assessment that can constitute some of the ingredients of a more structured analytical vulnerability assessment, based on engineering

principles. For instance a study at the urban scale can provide insight on the shape of single buildings and aggregate and hence an understanding of the interactions among buildings. Details on floor construction and layout, type and layout of masonry, presence of connections among walls, can lead the seismic assessor to a qualitative judgement of relative robustness and resilience of different construction solutions. It is however only when these details are interpreted within a mechanical framework and the relations among the parts expressed in mathematical terms that the relevance of the various parameters to the overall seismic behaviour can be established and the relative vulnerability of different objects quantified with a measured level of reliability. To achieve so, such information cannot be simply descriptive, but needs to be collected in a systematic way to be used in mathematical models. Moreover in order to correctly measure the level of uncertainty and hence reliability of the risk assessment of a particular urban centre, the sampling and data collection needs to follow some consistent rules.

The appropriate approach to a seismic risk assessment at territorial scale needs to address diverse issues, to balance the relative simplicity of the analysis vis-à-vis the variability in the building stock, so as to properly represent the diverse typologies present and hence accurately characterise the global vulnerability and cumulative fragility, while explicitly accounting for the uncertainties related to modelling limitation, the inherent randomness of the sample, and the randomness of the response.

For ordinary buildings seismic risk assessment is typically carried out for the performance condition of life safety and collapse prevention, related to a seismic hazard scenario related to a 10 % probability of exceedence in 50 year or 475 year return period. For historic buildings in city centre and in case of assets of particular value, it might be more appropriate to consider the performance condition of damage limitation or significant damage associated to lower-intensity and shorter return period seismic hazard. Recently has been argued by the author that for specific studies of high value historic buildings, such as the ISMEP project [1], and where sufficient information on the seismicity of the region is available, such as the case of Istanbul, a deterministic analysis can be used to define the hazard, rather than the probabilistic one, and consider the most credible seismic scenario within the set timeframe of assessment.

In the following sections of the chapter, after a review of earlier approaches to seismic vulnerability, the derivation of fragility functions is illustrated for three different methodologies: an empirical approach based on a modified version of the Vulnerability Index [2], an analytical approach based on mechanical simulation called FaMIVE [3] and a similar analytical approach for aggregates.

2 Vulnerability Assessment Methodologies

As stated in the introduction, when performing vulnerability assessment of large numbers of buildings and over an urban centre or a region, the resources and quantity of information required is large and thus the use of less sophisticated

and onerous inspection and recording tools is more practical. Methodologies for vulnerability assessment at the national scale should hence be based on few parameters, some of an empirical nature based on knowledge of the effects of past earthquakes, which can then be treated statistically.

In the recent past, European partnerships [4–6] constituting various work-groups on different aspects of vulnerability assessment and earthquake risk mitigation have defined, particularly for the former, methodologies that are grouped into essentially three categories in terms of their level of detail, scale of evaluation and use of data (first, second and third level approaches). First level approaches use a considerable amount of qualitative information and are ideal for the development of seismic vulnerability assessment for large scale analysis. Second level approaches are based on mechanical models and rely on a higher quality of information (geometrical and mechanical) regarding building stock. The third level involves the use of numerical modelling techniques that require a complete and rigorous survey of individual buildings. The definition and nature of the approach (qualitative and quantitative) naturally condition the formulation of the methodologies and the level at which the evaluation is conducted, from the expedite evaluation of buildings based on visual observation to the most complex numerical modelling of single buildings (see Fig. 1).

A most important criterion of distinguishing vulnerability approaches for historic buildings, is whether the method is purely empirical, i.e. based on observation and record of damage in past earthquake, from which a correlation between

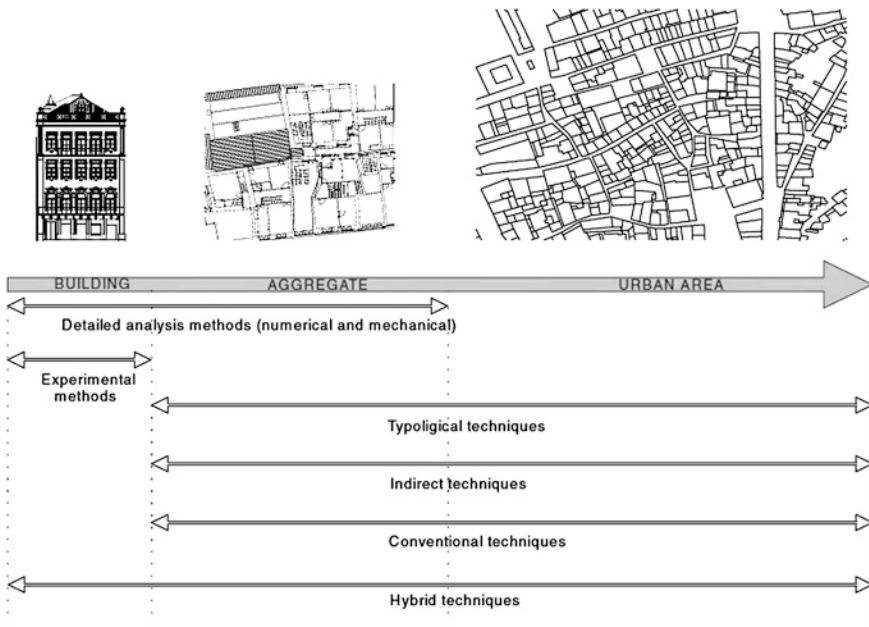


Fig. 1 Analytical techniques used at different evaluation scales

building typologies and damage level given a seismic intensity level can be derived, or analytical, where a model of a representative building for a typology is defined, and the response of such model to expected shaking intensities is computed. The first approach is particularly suited to historic city centres where a record of past earthquakes is available and damage to the building has been collected systematically over a number of events. This is for instance the case of the GNDT-AEDES approach developed in Italy over several decades from the earthquake in Friuli onwards [7]. The second approach is suitable to areas for which construction details are recorded and well understood, there might be some experimental work available to characterise their mechanical behaviour, there is some record of damage to calibrate the procedure, but most importantly they are suitable to be used to produce scenarios for future event and help define strengthening strategies, at the level of the single building, urban block, district or entire city [4].

A third approach is the heuristic or expert opinion approach by which vulnerability is attributed to building typologies by a panel of experts elicited to perform an assessment based on a common set of information and their previous knowledge. An example of such approach is the development of the vulnerability classes defined within the European Macroseismic Scale EMS-98 [8]. To the above three approaches a fourth, hybrid, can be added.

Following the first example of such classification developed by [8] and refined by [9], vulnerability approaches can also be grouped in direct and indirect. A brief review of the most significant approaches in each group is included in the remainder of this section.

Direct techniques use only one step to estimate the damage caused to a structure by an earthquake, employing two types of methods; *typological* and *mechanical*:

Typological methods—classify buildings into classes depending on materials, construction techniques, structural features and other factors influencing building response. Vulnerability is defined as the probability of a structure to suffer a certain level of damage for a defined seismic intensity. Evaluation of damage probability is based on observed and recorded damage after previous earthquakes and also on expert knowledge. Results obtained using this method must be considered in terms of their statistical accuracy, since they are based on simple field investigation. In effect the results are valid only for the area assessed, or for other areas of similar construction typology and equal level of seismic hazard. Examples of this method are the vulnerability functions or Damage Probability Matrices (DPM) developed by [9], in which a matrix for each building type or vulnerability class is defined that directly correlates seismic intensity with probable level of damage suffered.

Mechanical methods—predict the seismic effect on the structure through the use of an appropriate mechanical model, which may be more or less complex, of the whole building or of an individual structural element. Methods based on simplified mechanical models are more suitable for the analysis of a large number of buildings as require only a few input parameters, modest computing burden and can lead to reliable quantitative evaluations. A commonly used method belonging

to this group is the limit state method, based on limit state analysis (displacement capacity and demand) [10] applied this method to the analysis of the historic city centre of Catania considering only in plane mechanisms. The FAMIVE method [11] is a more holistic and reliable mechanically-based method, considering a suite of different mechanisms directly correlated to structural and constructional features. More sophisticated methods are generally used to evaluate single structures at a higher level of detail (in terms of building structure and construction) and are based on more refined modelling techniques. The analytical procedure for this type of method can involve non-linear static push over analysis such as the methodologies at [12, 13] and Capacity Spectrum Method (CSM) [14]. Examples of CSM application are provided in Sects. 3.2 and 3.3.

Indirect techniques initially involve the determination of a vulnerability index, followed by establishment of the relationships between damage and seismic intensity, supported by statistical studies of post-earthquake damage data. This form of evaluation is used extensively in the analysis of vulnerability on a wide scale. Of the various techniques currently available, the methodology initially developed by GNDT in the 1980s has undergone various modification and applications, for example Catania in 1999 and Molise in 2001 [7]. The method involves the determination of a building vulnerability classification system (vulnerability index) based on observation of physical construction and structural characteristics. Each building is classified in terms of a vulnerability index related to a damage grade determined via the use of vulnerability functions. These functions enable the formulation, of the damage suffered by buildings for each level of seismic intensity (or peak ground acceleration, PGA) and vulnerability index. These types of methods use extensive databases of building characteristics (typological and mechanical properties) and rely on observed damage after previous earthquakes to classify vulnerability, based on a score assignment. The rapid screening ATC-21 technique (1988) is extensively used in the U.S. to obtain such a vulnerability score [15]. An example of application of GNDT approach is shown in Sect. 3.1

Conventional techniques are essentially heuristic, introducing a vulnerability index for the prediction of the level of damage. There are essentially two types of approach: those that qualify the different physical characteristics of structures empirically and those based on the criteria defined in seismic design standards for structures, evaluating the capacity-demand relationship of buildings. ATC-13 [16], the best known of the first type, defines damage probability matrices for 78 classes of structure, 40 of which refer to buildings. Uncertainty is treated explicitly through a probabilistic approach. The HAZUS methods [17] belongs to the second type, providing parameters for capacity curves and damage through the CSM approach. Damage level are derived heuristically for 36 building classes [18]. For each construction type and level of earthquake-resistant design, the capacity of the structure, spectral displacement and inter-story drift limit are defined for different levels of damage.

Hybrid techniques combine features of the methods described previously, such as vulnerability functions based on observed vulnerability and expert judgment, in

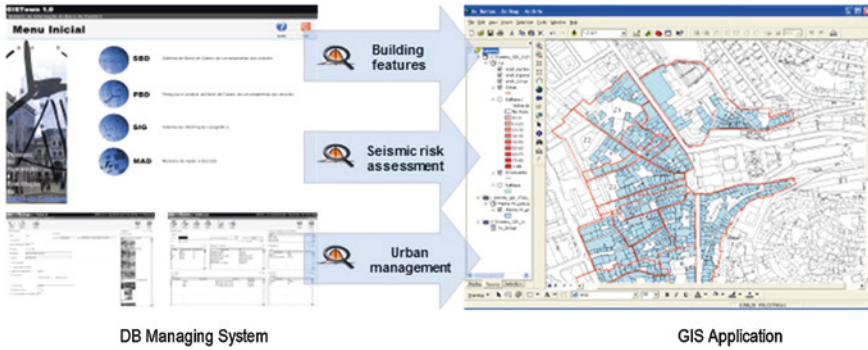


Fig. 2 Database and GIS framework (from [20])

which vulnerability is based on the vulnerability classes defined in the European Macroseismic Scale, EMS-98 [8]. This is the case in the Macroseismic Method devised by [19], which combines the characteristics of typological and indirect methods using the vulnerability classes defined in the EMS-98 scale and a vulnerability index improved by the use of modification factors.

For a robust decision making process following a risk analysis of a region it is essential to visualise and interpret the results considering their spatial distribution. The use of relational database within a GIS environment, allows to manage data regarding historic building stock characteristics, conservation requirements, seismic vulnerability, damage and loss scenarios, cost estimation and conduct risk-impact assessment.

Figure 2 represents such an application. Such platforms allow visualising both collected data and damage distributions for different hazard scenarios, and depending on the resolutions results can be mapped down to a single building.

3 Vulnerability of Historic Masonry Buildings

3.1 Empirical Approach

Historic masonry buildings do not have adequate seismic capacity and consequently require special attention due to their incalculable historical, cultural and architectural value. The amount of resources spent on their vulnerability assessment and structural safety evaluation is justifiable, since not only does a first level assessment [21, 22] include building inspection, but also can help in the identification of building for which a more detailed assessment is required, as well as the definition of priorities for both retrofitting and in support of earthquake risk management [23]. The definition and validation of a scoring method for the urban scale assessment of historic building is described in this section.

The methodology presented here can be classified as a hybrid technique. The vulnerability index formulation proposed is based essentially on the GNDT Level II approach [7] based on post-seismic damage observation and survey data covering a vast area, focussing on the most important parameters affecting building damage which must be surveyed individually.

Overall vulnerability is calculated as the weighted sum of 14 parameters (see Table 1) used in the formulation of the seismic vulnerability index. These parameters are related to four classes of increasing vulnerability: A, B, C and D. Each parameter represents a building feature influencing building response to seismic activity. A weight π_i is assigned to each parameter, ranging from 0.50 for the less important parameters (in terms of structural vulnerability) up to 1.5 for the most important (for example parameter P3 represents conventional strength) as shown in Table 1. The vulnerability index obtained as the weighted sum of the 14 parameters initially ranges between 0 and 650, with the value then normalised to fall within the range $0 < I_v < 100$. The calculated vulnerability index can then be used to estimate building damage due to a seismic event of given intensity.

This procedure has been used in Italy for the last 25 years and was later adapted by [24] for Portuguese masonry buildings and improved by: (i) introducing a more detailed analysis based on better data on the building stock; (ii) clarifying the definition of some of the most important parameters; and (iii) introducing new parameters that take into account the interaction between buildings (structural aggregates) and other overlooked building features. The addition of parameters P5, P7 and P10 provides: the height of the building (P5); the interaction between contiguous buildings (P7)—a very important feature when assessing buildings in urban areas; and the alignment of wall façade openings which affects the load path and load bearing capacity (P10).

The 14 parameters are arranged into four groups, as shown in Table 1, in order to emphasise their differences and relative importance (see [24]). The first group includes parameters P1 and P2 characterising the building resisting system, the type and quality of masonry, through the material (size, shape and stone type), masonry fabric, arrangement and quality of connections between walls; P3 roughly estimates the shear strength capacity; P4 evaluates the potential risk of out-of-plane collapse, P5 evaluate the height and P6 the foundation soil. The second group of parameters is mainly focused on the relative location of a building in the area as a whole and on its interaction with other buildings (parameter P7). This feature, not considered in other methodologies, is extremely important, since the seismic response of a group of buildings is rather different to the response of a single building. Parameters P8 and P9 evaluate irregularity in plan and height, while parameter P10 identifies the relative location of openings, which is important in terms of the load path. The third group of parameters, which includes P11 and P12, evaluates horizontal structural systems, namely the type of connection of the timber floors and the thrust of pitched roofing systems. Finally, P13 evaluates structural fragilities and conservation level of the building, while P14 measures the negative influence of non-structural elements with poor connections to the main structural system. As can be seen in Table 1, among all parameters, P3, P5

Table 1 Vulnerability index (I_v)

Parameters	Class C_{vi}				Weight P_i	Vulnerability index
	A	B	C	D		
1. Structural building system						
P1	0	5	20	50	0.75	$I_v^* = \sum_{i=1}^{14} C_{vi} \times P_i$
P2	0	5	20	50	1.00	
P3	0	5	20	50	1.50	
P4	0	5	20	50	0.50	
P5	0	5	20	50	1.50	
P6	0	5	20	50	0.75	
2. Irregularities and interaction						
P7	0	5	20	50	1.50	$I_v^* = \sum_{i=1}^{14} C_{vi} \times P_i$
P8	0	5	20	50	0.75	
P9	0	5	20	50	0.75	
P10	0	5	20	50	0.50	
3. Floor slabs and roofs						
P11	0	5	20	50	1.00	Normalised index $0 \leq I_v \leq 100$
P12	0	5	20	50	1.00	
4. Conservation status and other elements						
P13	0	5	20	50	1.00	Normalised index $0 \leq I_v \leq 100$
P14	0	5	20	50	0.50	

and P7 have the highest weight values (p_i) in the vulnerability index. On the other hand, parameter P2, P11, 12 and P13 are those whose increase could be defined as representing a strengthening action (masonry consolidation, timber floor stiffening, retrofitting of trussed roofing systems, effective connection between horizontal and vertical structural elements and building maintenance strategy).

The definition of each parameter weight is a major source of uncertainty as it is based on expert opinion. Consequently in order for the results to be accurately interpreted statistically, upper and lower bounds of the vulnerability index, I_v , were defined. This method can be considered robust when two conditions are verified: (i) the inspection of the majority of buildings under analysis was carried out in detail; and (ii) accurate geometrical information was available. A confidence level indicator is associated with each parameter, so that the vulnerability index is also coupled to a confidence level rating.

To resolve the conflict of a detailed inspection versus a large number of building to be inspected in an urban area a strategy is chosen to undertake a vulnerability assessment in two phases: in the first phase, an evaluation of vulnerability index, I_v , is made for those buildings for which detailed information is available—geometrical and morphological information, blue prints, survey sheets, etc. -; in the second phase a more expeditious approach is adopted, based on the mean values obtained from the first phase. The underlying assumption is that masonry building characteristics are homogeneous in the region under study. The mean vulnerability index value obtained for all masonry buildings in the first detailed evaluation is used as vulnerability index for a typology, to be weighed by modifiers for each building. Classification of these modifiers will affect the total vulnerability index computed in Table 1 as sum of all the weighed parameters, some of which act as modifiers of the mean score.

Table 2 presents the seven modifier parameters and their scores in relation to the average vulnerability value for each parameter. The vulnerability index, I_v , is defined according to the sum of the modifier parameter scores for each non-detailed assessment.

Table 2 Vulnerability modifier factors and scores

Vulnerability modifiers	Vulnerability classes, c_{vi}				Modified score: $\frac{p_i}{\sum_{i=1}^7 p_i} \times (c_{vi} - \bar{c}_{vi})$ p_i : parameter, i , weight assigned $\sum_{i=1}^7 p_i$: sum of parameter weights c_{vi} : modifier factor vulnerability class \bar{c}_{vi} : average vulner- ability class of parameter i
	A	B	C	D	
P5 Number of floors	-4.1	-3.1	0.0	6.2	
P6 Location and soil conditions	-0.5	0.0	1.6	4.7	
P7 Aggregate position and interaction	-1.0	0.0	3.1	9.3	
P8 Plan configuration	-2.1	-1.6	0.0	3.1	
P9 Regularity in height	-2.1	-1.8	0.0	3.1	
P12 Roofing system	-2.8	-2.1	0.0	4.1	
P13 Fragilities and conservation state	-2.8	-2.1	0.0	4.1	
Maximum modifier range, $\sum \Delta I_v$	-15.3	-10.3	4.7	34.7	

The scores for each parameter are defined with respect to the average value of that parameter obtained for the mean value of the vulnerability index and the weight of each parameter in the overall definition. For example, as the mean vulnerability class value for parameter P8 (plan configuration) obtained by the detailed assessment is taken as that of class C, the modifier scores are computed with respect to this average value. The final vulnerability is defined as:

$$\overline{I}_v = \overline{I}_v + \sum \Delta I_v \quad (1)$$

where \overline{I}_v is the final vulnerability index, \overline{I}_v is the average vulnerability index from the detailed assessment and $\sum \Delta I_v$ is the sum of the modified scores.

It is then possible to estimate damage associated with a certain level of seismic intensity, I , described in terms of macroseismic intensity [8]. The validation of this vulnerability index method was carried out by [21] through correlation between the GNDT II method [2] and the EMS-98 Macroseismic Scale, as indicated in [20]. On the basis of the EMS-98 scale damage definitions it is possible to derive damage probability matrices for each of the defined vulnerability classes (A–F). Through numerical interpretation of the linguistic definitions, Few, Many and Most, complete Damage Probability Matrices (DPM) for every vulnerability class may be obtained. Having solved the incompleteness using probability theory, the ambiguity and overlap of the linguistic definitions is then tackled using fuzzy set theory [25], by deriving, for each building typology and vulnerability class, upper and lower limits for the correlation between macroseismic intensity and mean damage grade.

For the operational implementation of the methodology, an analytical expression is proposed [26] which correlates hazard with the mean damage grade ($0 < \mu_D < 5$) of the damage distribution (discrete beta distribution) in terms of the vulnerability value, as shown in Eq. 2.

$$\mu_D = 2.5 + 3 \times \tanh \left(\frac{I + 6.25 \times V - 12.7}{Q} \right) \times f(V, I) \quad (2)$$

where I is the seismic hazard described in terms of macroseismic intensity, V the vulnerability index as calculated by [20], Q a ductility factor and $f(V, I)$ is a function of the vulnerability index and intensity. The latter is introduced in order to understand the trend of numerical vulnerability curves derived from EMS-98 DPMs for lower values of the intensity grades ($I = V$ and VI) where:

$$f(V, I) = \begin{cases} e^{\frac{V}{2} \times (I-7)} & I \leq 7 \\ 1 & I > 7 \end{cases} \quad (3)$$

This analytical expression derives from the interpolation of vulnerability curves calculated from the completed DPMs, as suggested in the EMS-98 scale. Used to estimate physical damage, this mathematical formulation is based on work previously proposed by [27]. The vulnerability index, V , determines the position of the

curve, while the ductility factor, Q , determines the slope of the vulnerability function (rate of damage increases with rising intensity). Regression analysis and parametric studies performed by [27] lead to a mean value of $Q = 3.0$ being suggested for masonry buildings of fairly ductile behaviour.

Based on the comparison between both the methods (see [21]), the following analytical expression for the vulnerability index, V , was derived:

$$V = 0.56 + 0.0064 \times I_v \tag{4}$$

Via this relationship, the vulnerability index, I_v , can be transformed into the vulnerability index, V (used in the Macroseismic Method), enabling the calculation of the mean damage grade through Eq. 2 and subsequently the estimation of damage and loss. For those buildings where detailed evaluation was not carried out, the mean vulnerability index can be defined as a function of the vulnerability classes defined in terms of the EMS-98 scale. In this case, the modifier parameters can also be expressed in vulnerability index V format, taking into account the I_v values re-defined in Eq. 4.

Once vulnerability has been defined, the mean damage grade, μ_D , can be calculated for different macroseismic intensities, using Eq. 2. Figure 3 shows one example of vulnerability curves for a mean value of vulnerability index, $I_{v,mean}$, as well as for the upper and lower bound ranges ($I_{v,mean} - 2\sigma_{I_v}$; $I_{v,mean} - 1\sigma_{I_v}$; $I_{v,mean} + 1\sigma_{I_v}$; $I_{v,mean} + 2\sigma_{I_v}$). From these mean damage grade values, μ_D , different damage distribution histograms for events of varying seismic intensity and their respective vulnerability index values can be defined, using a probabilistic approach. The most commonly-applied methods are based on the binomial probability mass function and the beta probability density function.

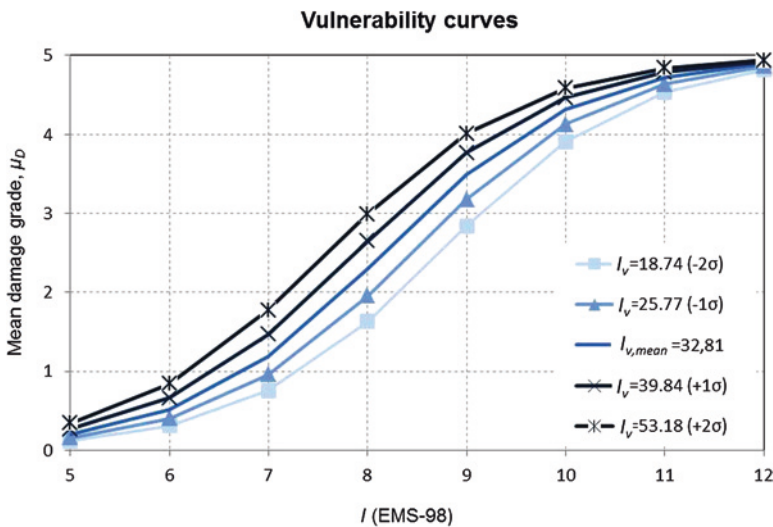


Fig. 3 Example of vulnerability curves for an old building stock

$$\text{PMF} : p_k = \frac{n!}{k!(n-k)!} \times d^k \times (1-d)^{n-k} \quad n \geq 0; 0 \leq p \leq 1 \quad (5)$$

The damage distribution fits to a beta distribution function, where t and r are geometric parameters associated with the damage distribution. Research carried out by [25] shows that the beta distribution is the most versatile, as variation of t and r enables the fitting of both very narrow and broad damage distributions. This continuous beta probability density function in which Γ is the known gamma function is expressed as:

$$\begin{aligned} \text{PMF} : p_\beta(x) &= \frac{\Gamma(t)}{\Gamma(r)\Gamma(t-r)} (x-a)^{r-1} (b-x)^{t-r-1} \\ &; a \leq x \leq b; a = 0; b = 5 \end{aligned} \quad (6)$$

Assuming that $a = 0$ and $b = 5$, it can then be simplified to:

$$\text{PMF} : p_\beta(x) = k(t,r) \times x^{r-1} \times (5-x)^{t-r-1} \quad (7)$$

where for a continuous variable x , the variance (σ_x^2) and the mean value (μ_x) of the values are related to t and r as defined below:

$$t = \frac{\mu_x(5 - \mu_x)}{\sigma_x^2}, \quad (8)$$

$$r = t \cdot \frac{\mu_x}{5} \quad (9)$$

The discrete distribution of the probability associated with each damage grade, D_k , with $k \in [0,5]$, is defined as:

$$\begin{aligned} P(D_0) = p(0) &= \int_0^{0.5} k(t,r) \cdot x^{r-1} (5-x)^{t-r-1} dx \\ P(D_k) = p(k) &= \int_{k-0}^{k-0.5} k(t,r) \cdot x^{r-1} (5-x)^{t-r-1} dx \\ P(D_5) = p(5) &= \int_{4.5}^5 k(t,r) \cdot x^{r-1} (5-x)^{t-r-1} dx \end{aligned} \quad (10)$$

For the definition of parameters t and r in the beta discrete distribution, the numerical damage distributions derived from the EMS-98 scale [26] can be used. The reduced variation obtained for parameter t in the numerical damage distributions justifies the adoption of a unique value of t (equal to 8) with which to represent the variance of all possible damage distributions. Based on this assumption, it is then possible to define the damage distributions exclusively through use of the

average value μ_D , characterized by variance coherent with that found via completion of the EMS-98 DPM's.

$$r = 8 \cdot \frac{\mu_D}{5} \tag{11}$$

Figure 4 presents examples of damage distributions obtained through use of the beta probability distribution ($t = 8$; $a = 0$; $b = 5$) for events of different seismic intensity and the mean value of the building vulnerability index ($I_v = 32.88$).

Another method of representing damage using damage distribution histograms involves the use of fragility curves. Here the probability of exceeding a certain damage grade or state, D_k ($k \in [0,5]$) is obtained directly from the physical building damage distributions derived from the beta probability function for a determined building typology. Just like the vulnerability curves, fragility curves define the relationship between earthquake intensity and damage in terms of the conditional cumulative probability of reaching a certain damage state. Probability histograms of a certain damage grade, $P(D_k = d)$, are derived from the difference of cumulative probabilities:

$$P(D_k = d) = P_D [D_k \geq d] - P_D [D_{k+1} \geq d] \tag{12}$$

Fragility curves are influenced by the parameters of the beta distribution function and allow for the estimation of damage as a continuous probability function. Figure 5 shows fragility curves corresponding to the damage distribution histograms of the mean vulnerability index value (I_v) as well as of the mean value plus one standard deviation ($I_v + \sigma_{I_v}$).

The next step in a risk assessment process is the estimation of losses. Loss estimation models can also be based on damage grades and involve correlating the probability of the occurrence of a certain damage level with the probability of building collapse and loss of functionality. The most frequently employed approaches are those based on observed damage data, such as the one proposed in [17] or that of the Italian National Seismic Survey. The latter was based on work by [28] which involved the analysis of data associated with the probability of

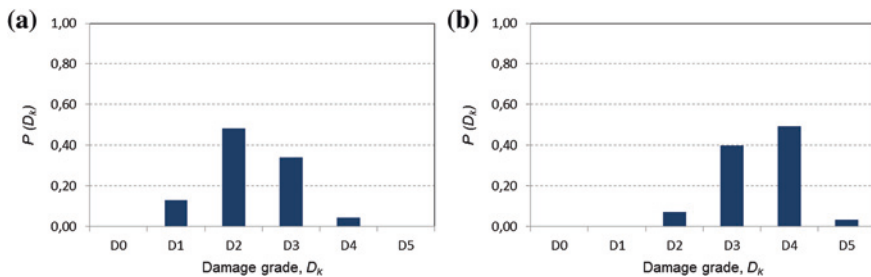


Fig. 4 Discrete damage distribution histograms for $I_v = 32.88$: **a** $I(EMS-98) = VIII$; **b** $I(EMS-98) = IX$

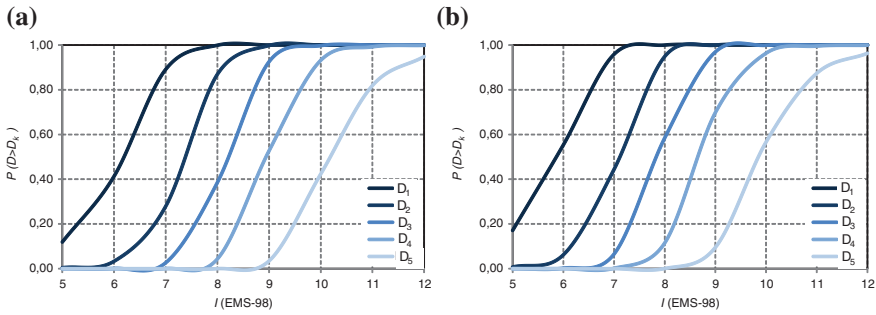


Fig. 5 From left to right: examples of fragility curves for I_v and $I_v + \sigma_{I_v}$

buildings to be deemed unusable after minor and moderate earthquakes. Although such events produce lower levels of structural and non-structural damage, higher mean damage values may occur which are associated with a higher probability of building collapse.

The probability of the occurrence of each damage grade is multiplied by a factor. This range from 0 to 1 and differs from proposal to proposal, based on statistical correlation. In Italy, data processing undertaken by [28] enabled the establishment of these weighted factors and respective expressions for their use in the estimation of building loss. For the analysis of collapsed and unusable buildings the following equations have been derived:

$$P_{collapse} = P(D_5) \tag{13}$$

$$P_{unusable\ buildings} = P(D_3) \times W_{ub,3} + P(D_4) \times W_{ub,4} \tag{14}$$

where $P(D_k)$ is the probability of the occurrence of a certain level of damage (D_1 to D_5) and $W_{ub,3}$, $W_{ub,4}$ are weights indicating the percentage of buildings associated with the damage level D_k , that have suffered collapse or that are considered unusable. The values of the weighting factors presented in the SSN [28] and [17] are slightly different. The weights: $W_{ub,3} = 0.4$; $W_{ub,4} = 0.6$; can be used for the evaluation of stone masonry buildings.

Figure 6 shows an example of probability curves which describe the results of building collapse and unusable building estimations for the mean value of the vulnerability index (I_v) as well as for other values of vulnerability, namely: ($I_{v,mean} - 2\sigma_{I_v}$; $I_{v,mean} - 1\sigma_{I_v}$; $I_{v,mean} + 1\sigma_{I_v}$; $I_{v,mean} + 2\sigma_{I_v}$).

One of the most serious consequences of an earthquake is the loss of human life and thus one of the major goals of risk mitigation strategies is ensuring human safety. Over the last hundred years the world has been struck by more than 1,250 strong earthquakes and over 1.5 million people have died as a consequence [29]. However official numbers are not always accurate and the actual totals may be much higher. Of the various casualty rate analyses and correlation laws found in the literature, those developed by [1, 29–31] are the most frequently cited.

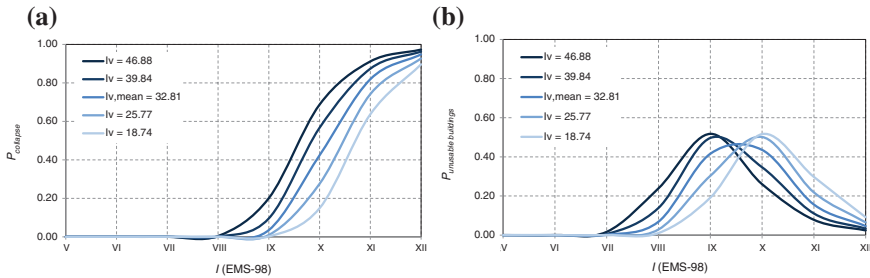


Fig. 6 Estimate of the collapsed and unusable buildings for different vulnerability values

Once again the Italian proposal [28] is presented here for consistency with the loss assessment procedure. The rate of dead and severely injured is projected as being 30 % of the residents living in collapsed and unusable buildings, with the survivors assumed to require short term shelter. Casualty (dead and severely injured) and homelessness rates are determined via Eqs. 15 and 16 respectively.

$$P_{dead\ and\ severely\ injured} = 0.3 \times P(D_5) \tag{15}$$

$$P_{homeless} = P(D_3) \times W_{ub,3} + P(D_4) \times W_{ub,4} + P(D_5) \times 0.7 \tag{16}$$

These two indicators are of great interest for risk management. Following the same logic, Fig. 7 shows an estimation of the numbers of dead, severely injured and homeless for the mean value of the vulnerability index (I_v), as well as for other vulnerability values ($I_{v,mean} - 2\sigma_{Iv}$; $I_{v,mean} - 1\sigma_{Iv}$; $I_{v,mean} + 1\sigma_{Iv}$; $I_{v,mean} + 2\sigma_{Iv}$).

Finally, the estimated damage grade can be interpreted economically, as defined by [2], i.e. the ratio between the repair cost and the replacement cost (building value). The correlation between damage grades and the repair and rebuilding costs are obtained by processing of post-earthquake damage data. As shown in Table 3, a variety of correlations are found in literature.

The most reasonable relationship, as confirmed by the post-seismic investigation of [32], is that which assumes a similar value of the damage index for damage

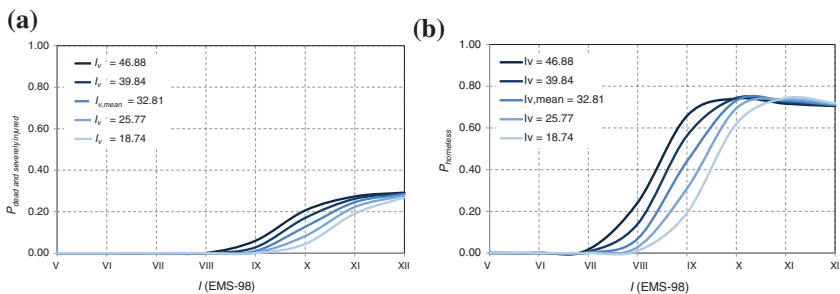


Fig. 7 Estimation of homeless and casualty rate for different values of vulnerability

Table 3 Correlation between damage levels and damage index

Damage grade, D_k	0	1	2	3	4	5
[28]	0.000	0.010	0.100	0.350	0.750	1.000
[16]	0.000	0.050	0.200	0.550	0.900	1.000
[31]	0.005	0.035	0.145	0.305	0.800	0.950

grade 4 and 5 and a greater difference between the damage index for the lower damage grades of 1 and 2. The values obtained by [16] and [31] are in agreement with these criteria. The statistical values obtained by these authors were derived from analysis of the data collected, using the GNDT-SSN procedure, after the Umbria-Marche (1997) and the Pollino (1998) earthquakes [31], and based on the estimated cost of typical repairs for more than 50,000 buildings.

The probabilities of the repair costs are defined as the product of the following two probabilities: The conditional probability of the repair cost for each damage level, $P[R|D_k]$, expressed by the values presented in Table 3, and the known conditional probability of the damage condition for each level of building vulnerability and seismic intensity, $P[D_k | v, I]$, given by:

$$Prob[R|I] = \sum_{D_k=1}^5 \sum_{I_v=0}^{100} Prob[R|D_k] \times Prob[D_k|I_v, I] \tag{17}$$

These values should be calculated for both the mean vulnerability index value and the lower and upper bound values ($I_{v,mean} - 2\sigma_{Iv}$; $I_{v,mean} - I\sigma_{Iv}$; $I_{v,mean} + I\sigma_{Iv}$; $I_{v,mean} + 2\sigma_{Iv}$). Note that according to this methodology, for seismic events of intensity in the range of V–IX the variation between estimated minimum and maximum repair cost is significant. For higher earthquake intensities, the difference is much smaller as a result of the high damage levels caused by severe seismic events.

3.2 Analytical Mechanical Approach: FaMIVE

The seismic vulnerability assessment of unreinforced masonry or adobe historic buildings can be performed with the Failure Mechanisms Identification and Vulnerability Evaluation (FaMIVE) analytical method, developed in [3, 33]. The FaMIVE method uses a nonlinear pseudo-static structural analysis with a degrading pushover curve to estimate the performance points by way of a variant of the N2 method [14], included in EC8 part 3 [34]. It yields as output collapse multipliers which identify the occurrence of possible different mechanisms for a given masonry construction typology, given certain structural characteristics.

Developed over the last decade, it is based on a suite of 12 possible failure mechanisms directly correlated to in situ observed damage [33, 35, 36] and laboratory experimental validation [37] as shown in Fig. 8.

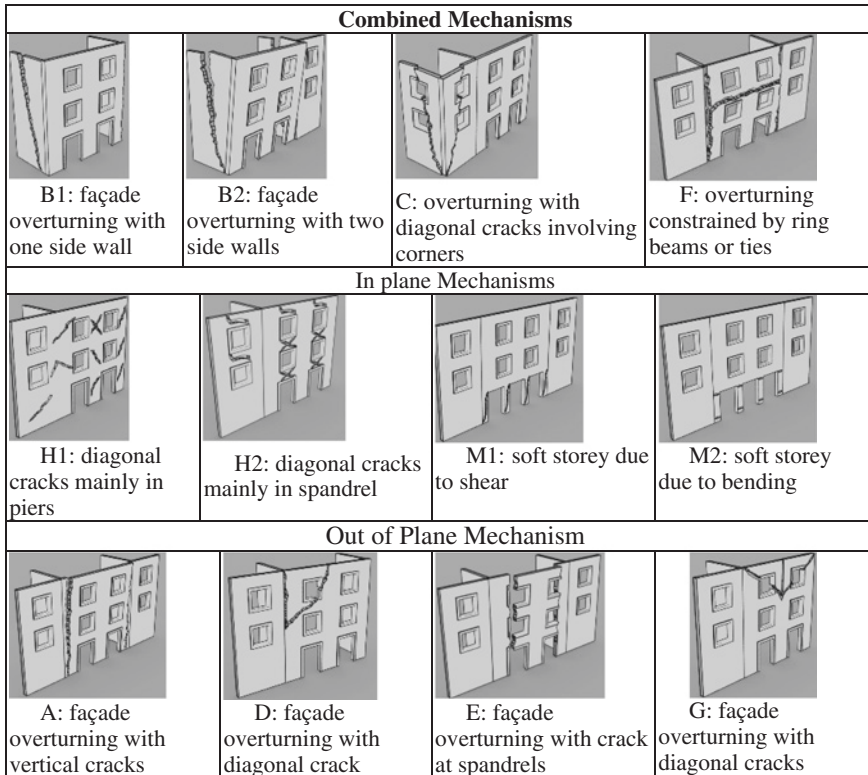


Fig. 8 Mechanisms for computation of limit lateral capacity of masonry façades

Each mode of failure corresponds to different constraints conditions between the façade and the rest of the structure, hence a collapse mechanism can be univocally defined and its collapse load factor computed. As shown in the flowchart of Fig. 9 the programme FaMIVE, first calculates the collapse load factor for each façade in a building, then taking into account geometric and structural characteristics and constraints, identifies the one which is most likely to occur considering the combination of the largest portion mobilised with the lowest collapse load factor at building level.

The FaMIVE algorithm produces vulnerability functions in terms of ultimate lateral capacity for different building typologies and quantifies the effect of strengthening and repair intervention on reduction of vulnerability. In its latest version it also computes capacity curves, performance points and outputs fragility curves for different seismic scenarios in terms of intermediate and ultimate displacements or ultimate acceleration. Within the FaMIVE database capacity curves and fragility functions are available for various unreinforced masonry typologies, from adobe to concrete blocks, for a number of reference typologies studied at sites in Italy [33, 36], Spain, Slovenia [38], Turkey [1], Nepal, India, Iran and Iraq. The procedure has been validated against the EMS-98 vulnerability classes [8, 26]

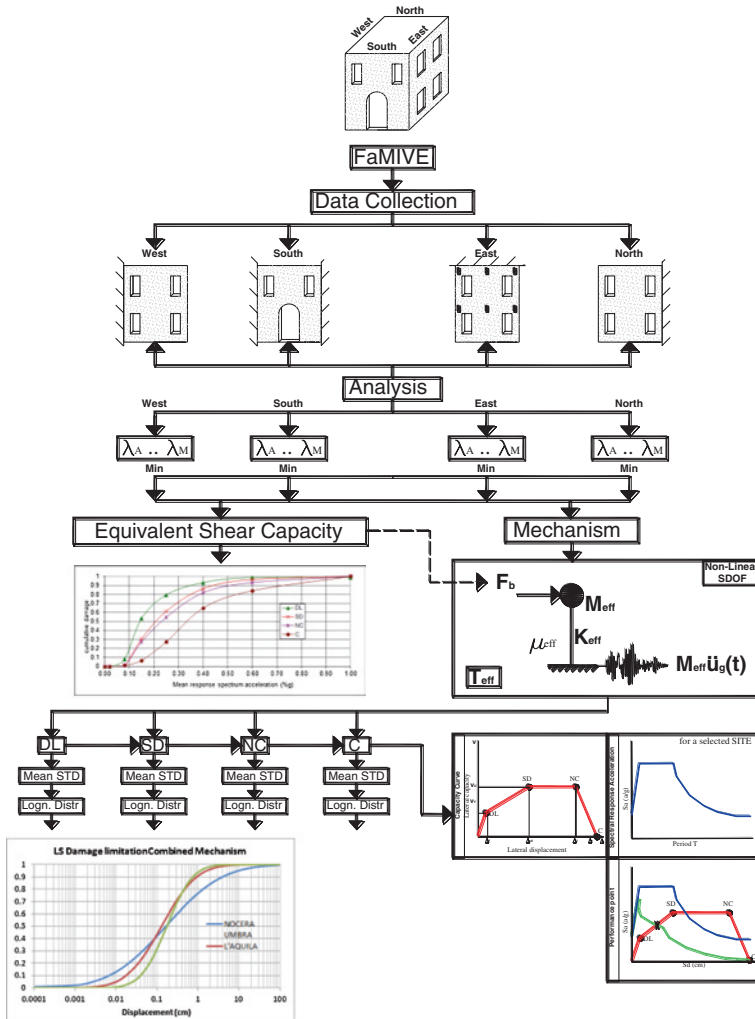


Fig. 9 Flowchart setting out the rationale of the FaMIVE Procedure

and recently used to produce capacity curves and fragility curves for use in the USGS PAGER environment [39, 40].

The mechanism’s characteristics are used to derive an equivalent non-linear single degree of freedom capacity curve to be compared to a spectrum demand curve, and eventually define performance points as illustrated in the flowchart in.

3.2.1 Definition of Damage Limit States and Damage Thresholds

In order to derive fragility curves the next step consist of defining limit state performance criteria to be correlated to damage states. This step is fraught with

uncertainties, as very limited consolidate evidence exist to perform such correlation over a wide range of building typologies and shaking levels. While robust database of damage states exist in literature no attempt has been so far made to record permanent drift and corresponding ground shaking in a consistent way, so as to provide empirical evidence for capacity curves. As an alternative, a number of authors have worked on correlating performance indicator and damage indicator on experimentally obtained capacity curves, by way of shaking table tests or push-over tests [41, 42]. The major limitation of these tests have been carried out focusing only on the capacity of in-plane walls, while very limited experimental work has been conducted on the characterisation of out-of-plane capacity for URM [43] have considered the out-of-plane failure of URM bearing walls constrained by flexible diaphragm, however the support conditions predefine the failure mode with three horizontal cylindrical hinges, already highlighted by [44], and rather different from on site and laboratory observation collected by [45]. A testing scheme more informed by observation of post-earthquake damage in existing masonry structures is the one devised by [46], however by predefining a state of damage the mechanism is also predefined.

Table 4 compares ranges for drift limit states as average from experimental literature, with the EC8 [34] provision for URM for the damage limit states of Significant damage and Near Collapse. The EC8 values relate to the in-plane failure of single pier elements, either with prevalent shear or flexural behaviour, while there is no indication for out of plane behaviour. In Table 4 are also included the range of values of performance drift obtained with the FaMIVE simulations for over 1000 cases as obtained from ten different sites for any type of masonry fabric and floor structure. The next section explains in detail how in the FaMIVE procedure the capacity curves are derived and the drift limit states computed.

Table 4 Performance drift value for damage limit states

Limit state		Damage limitation (%)	Significant damage (%)	Near Collapse (%)	Collapse (%)
<i>In-plane prevalent behaviour</i>	EC 8 Part 3		0.4–0.6	0.53–0.8	
	<i>Experimental</i>	0.18–0.23	0.65–0.90	1.23–1.92	2.1–2.8
	FaMIVE	0.023–0.132	0.069–0.679	0.990–1.579	1.801–2.547
<i>Out-of-plane prevalent behaviour</i>	EC8 Part 3		0.8–1.2 (H ₀ /D)	1.06–1.60 (H ₀ /D)	
	<i>Experimental</i>	0.33	0.88	2.3	4.8
	FaMIVE	0.263–0.691	0.841–1.580	1.266–1.961	2.167–5.562
<i>Combined prevalent behaviour</i>	FaMIVE	0.030–0.168	0.181–0.582	0.724–1.401	1.114–3.307

3.2.2 Derivation of Capacity Curves

Capacity curves can be derived for each façade on the basis of the following steps. The first step is to calculate the lateral effective stiffness for each wall and its tributary mass. The effective stiffness for a wall is calculated on the basis of the type of mechanism attained, the geometry of the wall and layout of opening, the constraints to other walls and floors and the portion of other walls involved in the mechanism:

$$K_{eff} = K_1 \frac{E_t I_{eff}}{H_{eff}^3} + K_2 \frac{E_t A_{eff}}{H_{eff}} \quad (18)$$

where H_{eff} is the height of the portion involved in the mechanism, E_t is the estimated modulus of the masonry as it can be obtained from experimental literature for different masonry typologies, I_{eff} and A_{eff} are the second moment of area and the cross sectional area, calculated taking into account extent and position of openings and variation of thickness over height, k_1 and k_2 are constants which assume different values depending on edge constraints and whether shear and flexural stiffness are relevant for the specific mechanism.

The tributary mass Ω_{eff} is calculated following the same approach and it includes the portion of the elevation activated by the mechanisms plus the mass of the horizontal structures involved in the mechanism:

$$\Omega_{eff} = V_{eff} \delta_m + \Omega_f + \Omega_r \quad (19)$$

where V_{eff} is the solid volume of the portion of wall involved in the mechanism, δ_m is the density of the masonry Ω_f, Ω_r are the masses of the horizontal structures involved in the mechanism. Effective mass and effective stiffness are used to calculate a natural period T_{eff} , which characterise an equivalent single degree of freedom (SDoF) oscillator:

$$T_{eff} = 2\pi \sqrt{\frac{\Omega_{eff}}{K_{eff}}} \quad (20)$$

The mass is applied at the height of the centre of gravity of the collapsing portion with respect to the ground and a linear acceleration distribution over the wall height is assumed. The elastic limit acceleration A_y is identified as the combination of lateral and gravitational load that will cause a triangular distribution of compression stresses at the base of the overturning portion, just before the onset of partialisation:

$$A_y = \frac{t_b^2}{6h_0} g \text{ with corresponding displacement}$$

$$\Delta_y = \frac{A_y}{4\pi^2} T_{eff}^2 \quad (21)$$

where, t_b is the effective thickness of the wall at the base of the overturning portion, h_o is the height to the ground of the centre of mass of the overturning portion, and T the natural period of the equivalent single degree of freedom (SDF) oscillator. The maximum lateral capacity A_u is defined as:

$$A_u = \frac{\lambda_c}{\alpha_1} \quad (22)$$

where λ_c is the load factor of the collapse mechanism chosen, calculated by FaMIVE, and α_1 is the proportion of total mass participating to the mechanism. This is calculated as the ratio of the mass of the façade and sides or internal walls and floor involved in the mechanism Ω_{eff} , to the total mass of the involved macroelements (walls, floors, and roof). The displacement corresponding to the peak lateral force, Δ_u is

$$3\Delta_y \leq \Delta_u \leq 6\Delta_y \quad (23)$$

as suggested by [47]. The range in Eq. (22) is useful to characterize masonry fabric of variable regularity and its integrity at ultimate conditions, with the lower bound better describing the behavior of adobe, rubble stone and brickwork in mud mortar, while the upper bound can be used for massive stone, brickwork set in lime or cement mortar and concrete blockwork.

Finally the near collapse condition is determined by the displacement Δ_{nc} identified by the condition of loss of vertical equilibrium which, for overturning mechanisms, can be computed as a lateral displacement at the top or for in plane mechanism by the loss of overlap of two units in successive courses:

$$\Delta_{nc} = t_b/3 \quad \text{or} \quad \Delta_{nc} = l/3 \quad (24)$$

where t_b is the thickness at the base of the overturning portion and l is the typical length of units forming the wall. In the case of in-plane mechanism the geometric parameter used for the elastic limit is, rather than the wall thickness, the width of the slender pier.

The thresholds points identified by Eqs. (20)–(23) can be associated to corresponding states of damage. Specifically **DL**, *damage limitation*, corresponds to the elastic lateral capacity threshold (D_y, A_y) defined by Eq. (20), **SD**, *significant damage*, corresponds to the peak capacity threshold (Δ_u, A_u) defined by Eqs. (21) and (22), and **NC**, *near collapse*, corresponds to incipient or partial collapse threshold (Δ_{nc}, A_u) defined by Eq. (23).

The procedure's approach also allows a direct analysis of the influence of different parameters on the resulting capacity curves, whether these are geometrical, mechanical or structural. By way of example Fig. 10 shows a comparison of average capacity curves grouping the results by different criteria for the same sample of buildings. In Fig. 10 the average curves are obtained by considering whether failure occurs by out-of-plane, in-plane or combined mechanism involving both sets of walls as presented in Fig. 8. In Fig. 11 the capacity curves are obtained by considering different structural typologies, as classified by the WHE-PAGER project [48] and shown in Table 5. It can be seen that the correlation between mode

Fig. 10 Average capacity curves for sample grouped by collapse mechanism classes

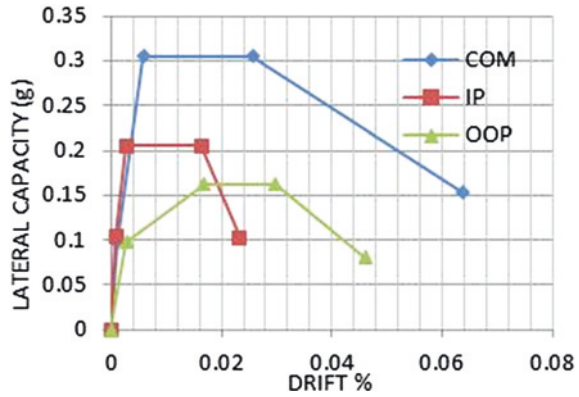


Fig. 11 Average capacity curves for sample grouped by structural typology

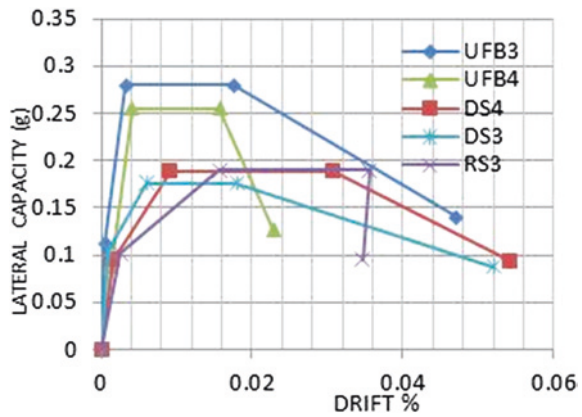


Table 5 Structural typologies classification according to PAGER [48]

Load bearing material	PAGER structure code	Description
Stone Masonry	RS3	Local field stones with lime mortar
	RS4	Local field stones with cement mortar, vaulted brick roof and floors
	DS2	Rectangular cut stone masonry block with lime mortar
	DS3	Rectangular cut stone masonry block with cement mortar
	DS4	Rectangular cut stone masonry block with reinforced concrete floors and roof
Brickwork or blockwork	MS	Massive stone masonry in lime or cement mortar
	UFB1	Unreinforced brick masonry in mud mortar without timber posts
	UFB3	Unreinforced brick masonry in lime mortar. Timber flooring
	UFB4	Unreinforced fired brick masonry, cement mortar. Timber flooring.
	UFB5	Unreinforced fired brick masonry, cement mortar, but with reinforced concrete floor and roof slabs
	UCB	Unreinforced concrete block masonry with lime or cement mortar

of failure and structural typology is qualitatively good but not univocal, and the grouping affects both ultimate lateral capacity and drift.

Substantial differences also exist for nominally the same structural typology from different regional setting. In Fig. 12 average capacity curves for structural typologies based on unreinforced brickwork with different mortars and horizontal structures are compared from different locations, one in Italy, one in Turkey, one in Nepal.

The results in Fig. 12 show that the parameter location, and hence construction details, layout and local tradition, might have a greater influence on the resulting curves, than the nominal structural typology class, usually considered of universal reference in many general purpose databases (such as HAZUS 99 [17], RISK-EU [5], LESS-LOSS [6], etc.). Such results bring in sharper focus the limitation and inaccuracy of using idealised models and average curves without adequately considering the inherent aleatoric variation associated with any given site where the assessment is conducted, and the importance of a detailed knowledge of the local construction characteristics when sampling the buildings representative of the building stock. A substantial variation in the drift associated with the various limit states can be also observed.

3.2.3 Performance Points and Their Correlation with Damage States

The lateral acceleration capacity and the relative proportion of drift for the three limit states identified in the previous section are essential indicators of the seismic performance. A method for assessing the overall behaviour by use of a global

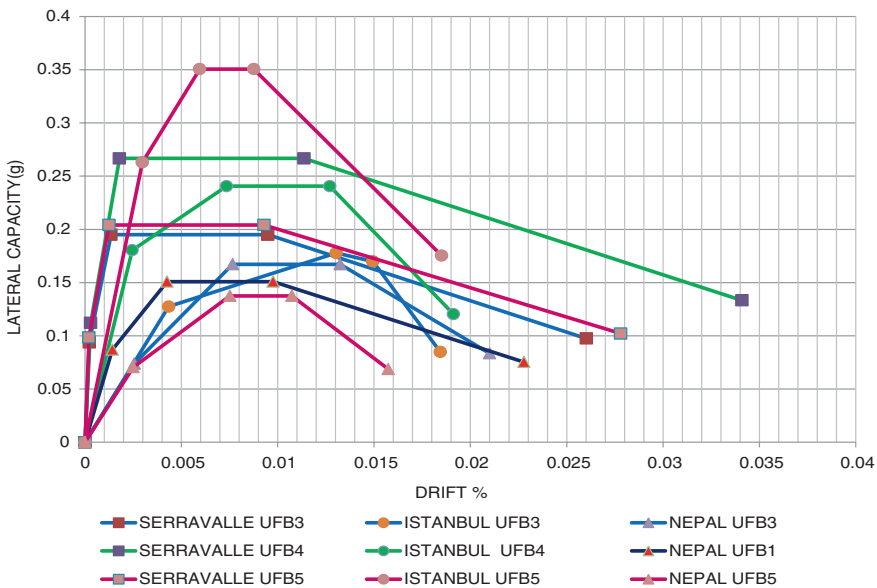


Fig. 12 Average capacity curves for different location and masonry typologies

performance indicator is the computation of the performance point. In order to calculate the performance point it is necessary to intersect the capacity curve derived above with the demand spectra for different return periods in relation to the performance criteria considered. Two broadly equivalent approaches for the derivation of the non-linear demand spectra exist: the N2 method [14] included in the EC8 [34] and the Capacity Spectrum method (CSP) [14]. The two methods differ essentially in the way the non-linear demand spectrum is arrived at: the N2 method uses a reduction factor R , function of the structure expected ductility μ , while the CSP uses a fictitious damping factor derived from the hysteresis loop of the structure. There exists a rich literature that compares the benefits of the two approaches [49]. In the following the N2 method will be used to illustrate the derivation of performance points.

To calculate the coordinates of the performance point in the displacement-acceleration space, the intersection of the capacity curve with the nonlinear demand spectrum for an appropriate level of ductility μ can be determined as shown in Eq. (24), given the value of A_u :

$$\begin{aligned}
 & \text{if } T < T_c \\
 & \text{if } A_u \geq A_{nl}(T) \Rightarrow SD_{nl}(\mu) = \frac{T_c^2 (\beta A_{el}(0) - A_{nl}(T))^2}{(\mu - 1)^2} * \frac{g\mu}{4\pi^2 A_{nl}(T)} \\
 & \text{if } A_{nl}(T_c) < A_u < A_{nl}(T) \Rightarrow SD_{nl}(\mu) = \frac{T_c^2 (\beta A_{el}(0) - A_u)^2}{(\mu - 1)^2} * \frac{g\mu}{4\pi^2 A_u} \\
 & \text{if } A_u \leq A_{nl}(T_c) \Rightarrow SD_{nl}(\mu) = \frac{gT_c^2 (\beta A_{el}(0))^2}{4\pi^2 \mu A_u} \tag{25} \\
 & \text{if } T \geq T_c \\
 & \text{if } A_u \geq A_{nl}(T) \Rightarrow SD_{nl}(\mu) = \frac{gT_c^2 (\beta A_{el}(0))^2}{4\pi^2 \mu A_{nl}(T)} \\
 & \text{if } A_u < A_{nl}(T) \Rightarrow SD_{nl}(\mu) = \frac{gT_c^2 (\beta A_{el}(0))^2}{4\pi^2 \mu A_u}
 \end{aligned}$$

where two different formulations are provided for values of ultimate capacity A_u greater or smaller than the nonlinear spectral acceleration $A_{nl}(T_c)$ associated with the corner period T_c marking the transition from constant acceleration to constant velocity section of the parent elastic spectrum. In (24) SD_{nl} is the non-linear spectral displacement, function of the chosen target ductility μ ; β is the acceleration amplification factor calculated as the ratio of the elastic maximum spectral acceleration and the peak ground acceleration $A_{el}(0)$; $A_{nl}(T)$ is the non-linear spectral acceleration for the value of natural period that defines the elastic branch of the capacity curve; g is the gravity constant. Note that in Eq. (24) $A_{el}(T)$, $A_{nl}(T)$ and A_u are dimensionless quantities, expressed as proportion of g .

In Fig. 13 the damage thresholds for the limit state of near collapse for each building in the sample of Nocera Umbra, Italy, are compared with the regional response spectrum for 475 year return period (or 10 % of exceedance in 50 years)

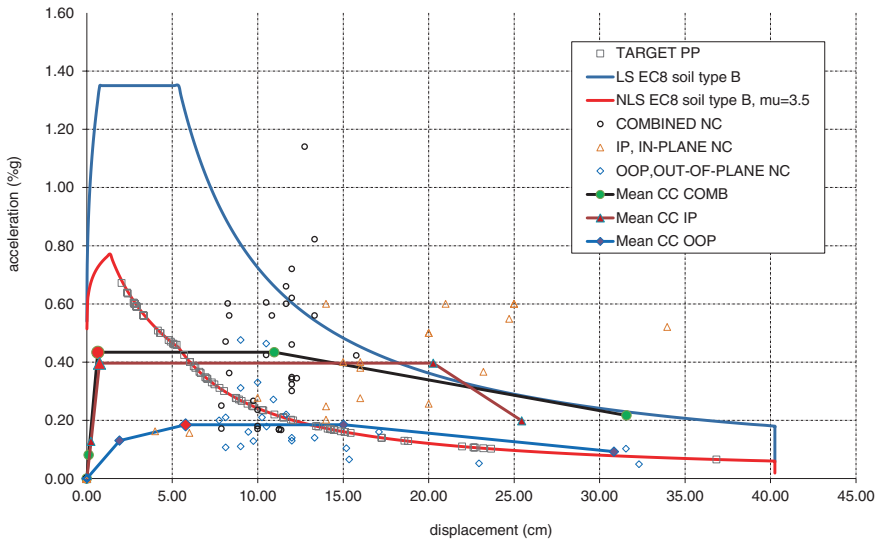


Fig. 13 Representation of target performance points and damage thresholds for Near Collapse limit states in the acceleration/displacement space. The PGA is the value recorded for the 1997 Umbria Marche earthquake in Nocera Umbra. On the mean capacity curve for the three mechanism classes, the mean significant damage thresholds are marked in *red*

anchored to the PGA of the second shock of the Umbria-Marche September 1997 sequence. For the non-linear spectrum obtained with the N2 method approach a ductility $\mu = 3.5$ has been chosen in agreement with experimental evidence provided by [47] and [50] and to match the performance point of NC for the mean capacity curve for the combined mechanism. It can be seen that there is quite a significant scatter of performance and most of the out-of plane mean curves lies below the nonlinear spectrum, meaning that a higher level of ductility is required to meet the performance.

It should also be noted that a consistent proportion of the representative points of Near Collapse lies under the nonlinear response spectrum, equally deficient in terms of acceleration and displacement, especially for the out of plane behaviour. Such outliers should not be overlooked as they usually point out to inherent construction deficiency in a regional context, inhibiting seismic resilience.

3.2.4 Derivation of Fragility Curves

Advanced uncertainty modelling and probability of occurrence of given phenomena is usually confined to the hazard component of the risk equations, while when probabilistic models are developed for vulnerability components, these usually relate to simplified modelling of the structure seismic response and assumption of pre-determined dispersion as might be found in literature [17, 51].

Usually it is also assumed that fragility curves for different limit states can be obtained by using mean values of the performance point displacement and deriving lognormal distributions by either computing the associated standard deviation if some form of random sampling has been considered, or by assuming values of β from empirical distribution or literature. To this end the average displacement for each limit state can be calculated as:

$$\bar{\Delta}_{LS} = e^{\mu} \text{ with } \mu = \frac{1}{n} \sum (\ln x) \tag{26}$$

and the corresponding standard deviation as:

$$\beta_{LS} = e^{\mu + \frac{1}{2}\sigma^2} \sqrt{e^{\sigma^2} - 1} \text{ with } \sigma = \sqrt{\frac{\sum (\ln x - \ln \bar{x})^2}{n}} \tag{27}$$

Figures 14 and 15 show the set of fragility curves obtained for each of the damage limit states of DL and SD as computed for the two Italian sites of Nocera Umbra and Serravalle considering separately the three types of structural behaviour. As, once a structural typology has been assigned, the values of the mechanical characteristics are the same across the two samples, while the structural details are accounted for directly in the three classes of mechanisms, the variability observed in each chart between samples can be related directly to geometric

Fig. 14 Fragility distribution for limit state of damage limitation for the three classes of collapse mechanisms for two different Italian sites

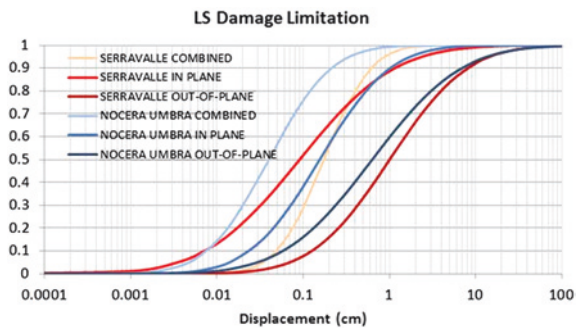
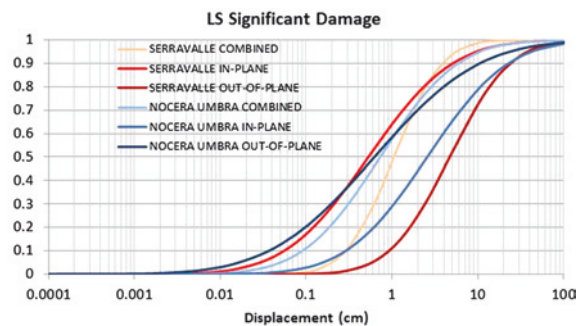


Fig. 15 Fragility curves for limit state of significant damage for two Italian samples for the three classes of collapse mechanism



differences and masonry fabric, i.e. to the local aspects of the construction practice and architectural layout. Hence curves on the left of the diagrams are stiffer in the case of damage limitation or have lesser ductility in the case of significant damage. However the distribution does not bare consistency across the three classes of mechanism for the two sites.

Figures 16 and 17 show the fragility distribution at ultimate conditions in terms of near collapse displacement and ultimate lateral capacity for the three failure behaviour. While there is little difference among the two locations for the out-of plane behaviour both the in-plane and the combined behaviour show high variability. The higher deformability of Serravalle for the in-plane behaviour is related to a higher proportion in this sample of facades with porticoes at ground level, resulting in possible soft storeys, while the lower value of limit displacement for the Nocera Umbra sample is dependent on a high proportion of masonry fabric of poorly hewed stone classified as RS3. On the other end the lower lateral capacity of the Serravalle sample for the combined mechanism is to be associated with slenderer façades. Moreover Nocera Umbra has a greater lateral capacity both for combined mechanisms and for in-plane mechanism than Serravalle (see Fig. 17) while ultimate capacity for the out-of-plane mechanism provides similar fragility curves.

The reliability of the results obtained in the previous section can be considered within the framework set out in the Eurocode 8 [34], whereby the reliability associated to the results of a seismic assessment of a structure is expressed as a

Fig. 16 Fragility curves for the limit state of near collapse for two Italian sites and three classes of mechanisms

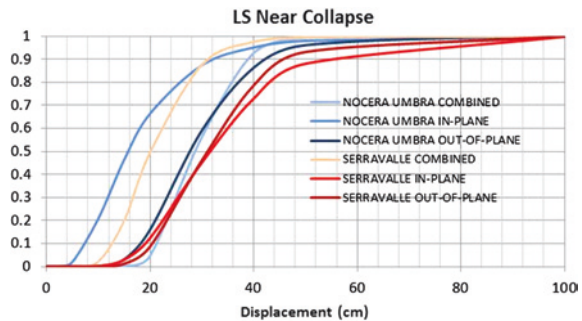
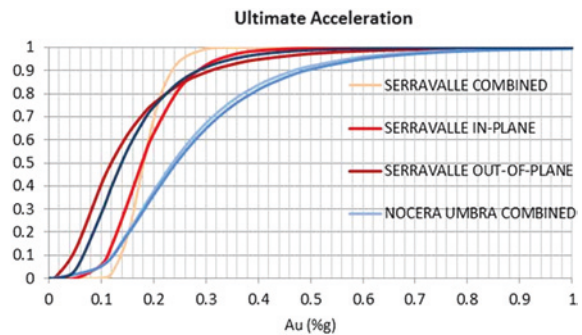


Fig. 17 Fragility curves for the ultimate lateral capacity for two Italian sites and three classes of mechanisms



function of the level of knowledge and quantified by means of the confidence factor. Hence this can be considered a measure of the epistemic uncertainty. Eurocode 8 recognises three levels of knowledge: limited, normal and full; and three fields of knowledge: geometry, construction details and materials. As data used in the FaMIVE approach are collected by on site visual inspection with some measurement and in situ accurate observation of construction details, while only very limited in situ non-destructive test on materials are performed and material characteristics are otherwise assigned based on literature or surveyor experience, then the level of knowledge is superior to KL1, *limited*, but not quite equal to KL2, *normal*. For this level of knowledge, a static nonlinear analysis, such as the limit state mechanism approach, leading to a capacity curve is deemed appropriate. Hence according to the recommended values the confidence factor CF should be in the range 1.2–1.35 depending on how closer the actual knowledge can be considered to the reference level identified by KL2. The confidence factor is then used in EC8 to reduce the capacity values as obtained from the assessment.

Although the EC8 approach recognise the importance of treating epistemic uncertainties, the level of knowledge is translated in a safety factor value rather than a probability or possibility of a specific value to occur. While this approach can be considered acceptable for the assessment of single buildings, it does not account explicitly for aleatoric variation.

The FaMIVE procedure uses a measure of reliability of the input data to determine the reliability of the output. Depending on whether data, in each section of the data collection form, has been collected and measured directly on site, or collected on site and confirmed by existing drawings or photograph, or collected from photographic evidence only, three level of reliability are considered, as high, medium and low, respectively, to which three confidence ranges of the value given for a parameter can be considered corresponding to 10 % variation, 20 % variation and 30 % variation. The parameter value attributed during the survey is considered central to the confidence range so that the interval of existence of each parameter is defined as $\mu \pm 5\%$, $\mu \pm 10\%$, $\mu \pm 15\%$, depending on highest or lowest reliability. The reliability applied to the output parameters, specifically lateral acceleration and limit states' displacement, is calculated as a weighted average of the reliability of each section of the data form, with minimum 5 % confidence range to maximum 15 % confidence range.

To quantify the effect of the level of the epistemic uncertainty on the fragility curves obtained with the FaMIVE procedure, the samples from three different locations in Italy and for the three failure behaviours introduced in the previous section, are analysed together. For each entry in the sample a separate reliability parameter is computed as indicated above, then two new sets of values representing the lower bound and upper bound for each entry are computed. For these two sets logarithmic mean and standard deviation are calculated using Eqs. (25) and (26) and the lognormal distributions obtained. These are presented in

Figure 18 for the three displacement limit states and for the ultimate acceleration, respectively. The reliability indicator for the overall sample is $\pm 11\%$, showing that the data reliability is medium–low, i.e. no availability of drawings in most

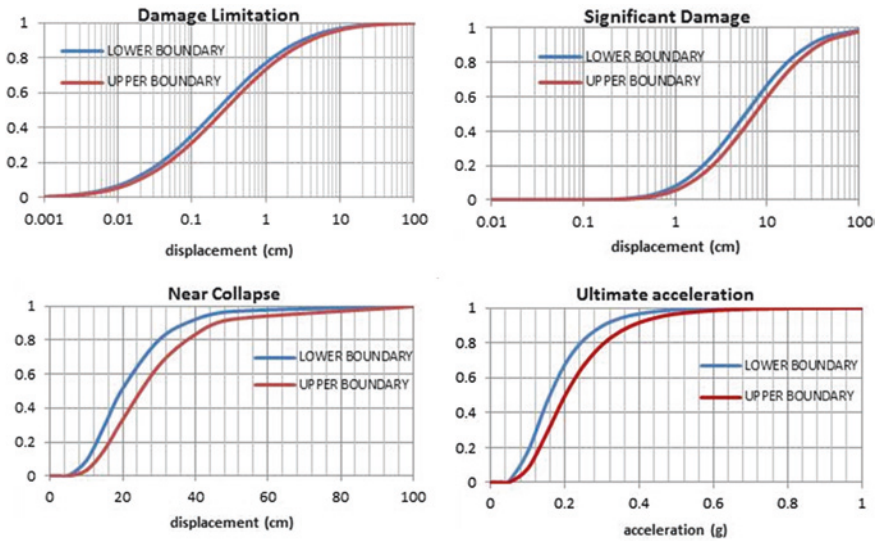


Fig. 18 Effect of epistemic uncertainty on fragility distribution for limit states

cases and onsite measurement on a modest number of cases. This is a typical situation in the aftermath of an earthquake, such as the conditions in which both the Nocera Umbra sample and the L'Aquila sample were collected.

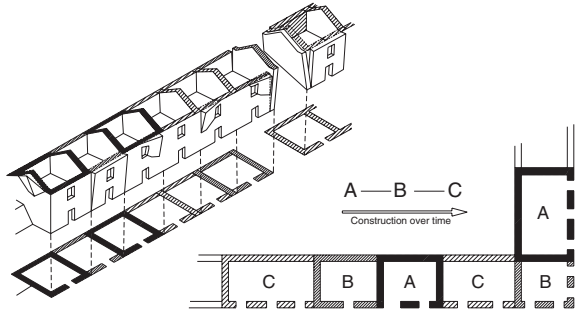
3.3 Building Aggregates

In historic centres the evolution of the urban layout is a critical factor. The diachronic process of construction means that in some cases adjacent buildings share load-bearing masonry walls and their façades are aligned. In this case, buildings do not constitute independent units, resulting in their structural interaction, particularly critical for horizontal actions. Hence the structural performance should be studied at the level of the aggregate and not only for each isolated building.

This chapter presents an extension of the mechanical methods introduced in the previous chapter, to undertake vulnerability assessment, evaluate seismic risk and estimate loss at the urban scale for historic city centres in which the building stock is structurally linked. It is assumed that collapse or ultimate limit state of the structure is due to shear-type failure.

A building aggregate can be considered as a unit, for which it is fundamental, the knowledge on building typology, conservation state and connection scheme between buildings, as a consequence of the evolution of the urban layout (see Fig. 19). The building interaction does not only change the load paths, but also the global and local seismic response, as a consequence of the quality of the connections. The vulnerability assessment for single buildings overlooks the integrity

Fig. 19 Diachronic construction process and building interaction (adapted from [50])



of the aggregate whether it is small or large aggregate, the irregularity created by confining buildings, connection to neighbouring buildings, etc. [50].

The interaction of buildings is first of all very dependent on irregularity raised by differences in height and stiffness of neighbouring buildings. Since the aggregate is constituted by single buildings, which have different level of vulnerability when considered individually, the position and layout of these can increase or reduce the vulnerability of the aggregate as a whole. In this sense the aggregate is a structural unit and should be evaluated as a global structure and from its collective behaviour and response to seismic action more vulnerable buildings can benefit from this confinement, however the interaction of the buildings can worsen the global vulnerability of an aggregate due to changes in height or stiffness. In general the global behaviour is beneficial for the more vulnerable buildings while for the stiffer units the level of damage suffered during a seismic event is greater, due to the interaction of strong building-weak building.

Building aggregates can take a number of shapes, as shown in Fig. 20, although buildings in a row are very characteristic of the eighteenth century urban layout for many European historic city centres. Whatever the aggregate shape, the seismic behaviour is evaluated in two main directions: parallel to the building façades development and perpendicular to them. More complex aggregate shapes can be sub-divided in smaller aggregates of simpler shape.

For the case of a row of buildings, many situations can arise from the interaction among buildings. Normally flexural failure is expected for buildings with slender masonry piers at ground floor due to big openings and shear failure for buildings with thick masonry piers between openings, but these kind of failure modes are altered because of the group response. The misalignments of building front, misalignments of window openings of adjacent buildings, big differences in wall area and stiffness of aligned buildings may change completely the load paths for the horizontal forces and the resulting failure mechanism.

Figure 21 shows an example of the influence of aggregate's layout on building failure mechanisms

It is often noted that end buildings are very vulnerable due to their position and normally suffer most damage by rotation and sliding phenomenon's induced by inertial forces of the whole aggregate in one direction. Furthermore the rigidity of timber diaphragms of masonry buildings do not oppose to the global behaviour



Fig. 20 Building aggregate shapes

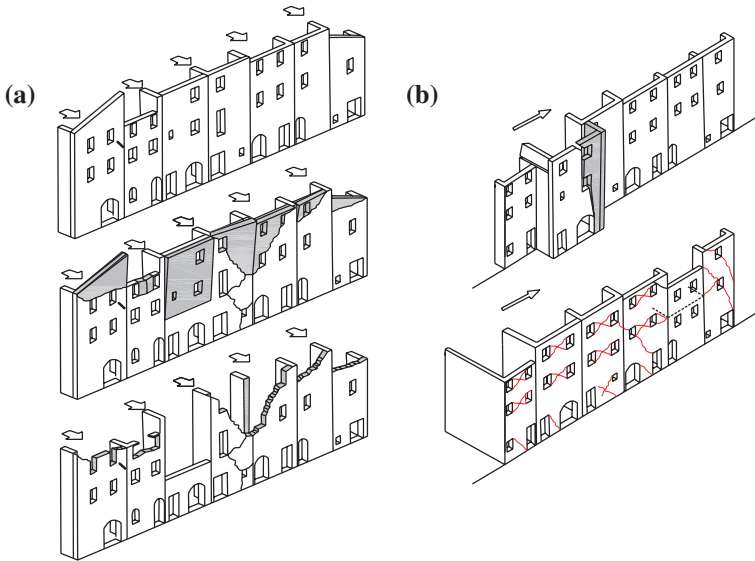


Fig. 21 Building interaction: a Out-of-plane; b In-plane

since they are flexible diaphragms but are important in the horizontal load distribution among masonry shear walls. In this direction the global response is proven to be of great importance, however in the perpendicular direction, the building response is substantially self-ruling. The masonry mid-walls of adjacent buildings, lacking openings, charged by floor structures leading to high values of normal stress appear to have high shear strength in the in-plane response and do not condition building failure. A critical issue for the facades of the aggregates, often observed in post seismic survey, is the out of plane collapse of walls. The weak connections to orthogonal walls, due to the building process of buildings in-between existent ones or to the addition of extra floor on the other may compromise the quality of connections among orthogonal walls. Out of plane collapses at roof level are also common due to the combined effect of weak connections and low values of normal stress reducing the shear capacity.

3.4 Mechanical Method for Building Aggregate

The vulnerability assessment procedure is based on the use of a simplified capacity curve for each building. To better understand the assessment process, it has been broken down into steps following the same logic as in Sect. 3.

3.4.1 Identification of Building Typology

A subdivision into two different typologies relating to two different wall arrangements are identified as A and B. This division is necessary to identify primarily the more vulnerable direction of the masonry building and define a more probable collapse mechanism as shown in Fig. 22:

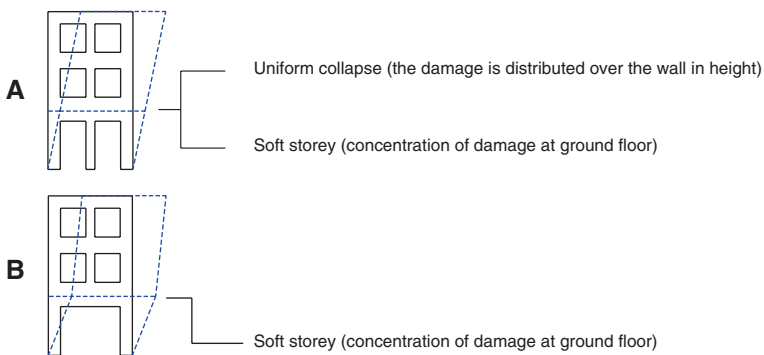


Fig. 22 Building typology and collapse mechanism

Type A—Masonry walls that have regular openings in height or few or no openings whatsoever (midwalls, gable end walls)

Type B—Masonry walls with big openings at ground floor level: This situation is a frequent characteristic in the refurbishment and transformation of historic masonry buildings where wall are suppressed to create larger open spaces.

3.4.2 Collapse Mechanism

The building aggregate is analysed considering two possible mechanisms: uniform collapse and soft-storey collapse. For each of the building typologies identified and relative to the direction considered, the analysis of a building or a group of buildings is undertaken considering the collapse mechanism and the typology. The following situation can be identified (see Fig. 22):

- For buildings of typology A, two collapse mechanisms are possible: the uniform collapse considers that the damage is distributed over the height of the wall and for the soft storey mechanism damage is concentrated at ground floor.
- For buildings of typology B only one collapse mechanism is considered because of its increased vulnerability at ground floor level.

3.4.3 Vulnerability Assessment

To evaluate the response of building aggregate with a bulky or array shape, in both principal directions (X, Y) it is assumed that the X-direction is the weaker direction of the building aggregate for which the occurrence of a soft storey mechanism is prevalent, for both building types A and B. For the other direction, Y, both collapsed mechanisms are considered in the assessment.

In an array of buildings the YY direction assumed as the stronger, is usually the direction of the majority of the party walls between buildings within the aggregate. These walls are assumed to have individual response. This hypothesis is fairly acceptable, because in this direction buildings do not interact as strongly as in the other direction (façade walls). In this direction a very straightforward vulnerability assessment is attained for each building using the mechanical model in which the simplified bilinear capacity curve (SDOF system) is constructed for each building [51, 53], limit states and the level of seismic action are defined, hence the performance point is retrieved through the capacity spectrum methodology (see [24]). Once the fragility curves for the four damage states are obtained, the evaluation of the probabilistic damage distribution is performed. The damage distribution of the aggregate in this direction is evaluated by the average value of the single damage distribution for each building for both collapse mechanisms (uniform collapse and soft storey mechanism), defining in this way a damage range for the building aggregate in this direction, without considering the damage of each building within the aggregate.

For the *XX* Direction, considered the weaker direction as mentioned, usually building façades are aligned and the interaction between buildings in this direction is much more important. The procedure adopted in this case is as follows:

- (i) Construction of each simplified bilinear capacity curve corresponding to a single degree of freedom system for each building in this direction. Once obtained these simplified capacity curves, they can be transformed into force–displacement curves and summed to obtain a global push-over curve for the aggregate. But since aggregates are formed by buildings with different height, horizontal displacements should be normalized in such a way that $\phi_n = 1$ (modal shape vector), where *n* is the control node. This must be done because buildings that compose and aggregate have different number of floors and consequently different height and therefore top-displacement at roof level that is normally considered cannot be the selected control node. To achieve this, the displacements are divided by the number of floors, therefore the control node is the displacement at ground floor and the curves can be summed (see Fig. 23). Each simplified capacity curve (*Ay*, *dy*, *du*) is then normalized by transformation of coordinates into the force–displacement using the following expressions:

$$\text{Force : } F = Ay \times m \cdot \Gamma \tag{28}$$

$$\text{Displacement : } d = \frac{dy \times \Gamma}{N}; \quad N : \text{numt} \tag{29}$$

- (ii) The force displacement curves are summed and the global pushover curve of the building aggregate is obtained in this direction (see Fig. 23)

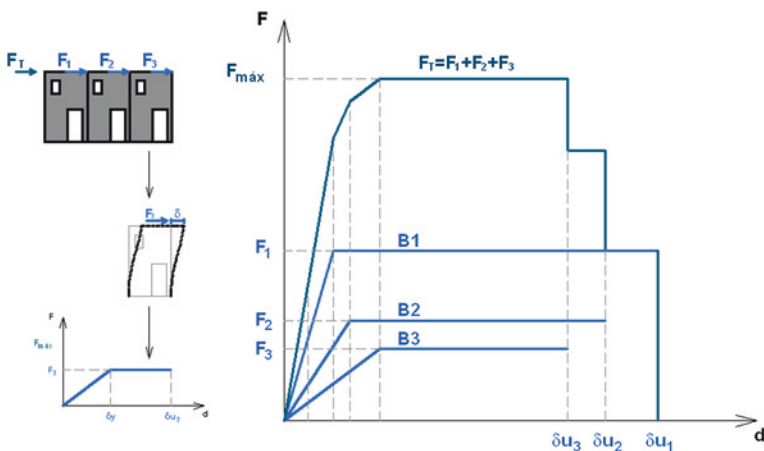


Fig. 23 Construction of the global push-over curve

(iii) The determination of an equivalent elasto-perfectly plastic force–displacement relationship for the building aggregate is constructed (non-linear static analysis through a simplified mechanical model) that the elastic stiffness of an equivalent bilinear system is found by marking the secant to the push-over curve at the point corresponding to a shear base 70 % of the maximum value (maximum base shear). The horizontal section of the bilinear curve shall be found by equalizing the areas underneath the two curves up to the ultimate displacement of the system. The value of the ultimate displacement which is considered equal to the ultimate limit state corresponds to a force degradation of not more than 20 % of the maximum. The construction of the equivalent global pushover curve, an equivalent capacity curve to evaluate the response of the aggregate structure must take into account two possible situations:

- (a) There is no building within the aggregate that collapses of a value of shear base 70 % of the maximum shear of the global pushover curve and in this case the equivalent bilinear curve is defined analytically as followed in Fig. 24.
- (b) If a building within the aggregate collapses before attaining the 70 % of the maximum shear value defined for the global push-over curve, it will drop of a value of the shear capacity of the building that prematurely failed. In this case, the equivalent stiffness is found by marking the secant to the unfailed push-over curve and the horizontal section is defined as

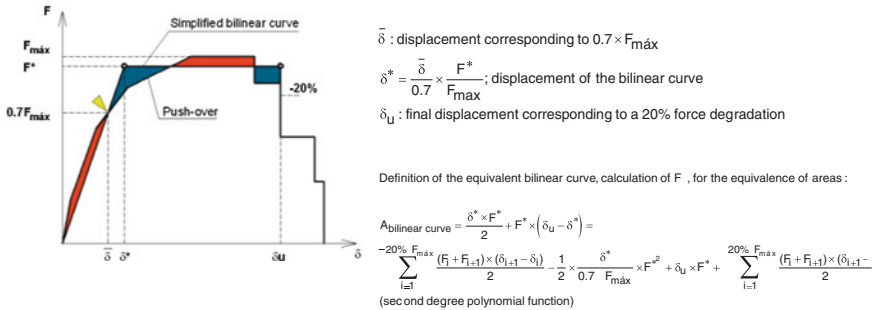


Fig. 24 Construction of the equivalent bilinear curve—case a)

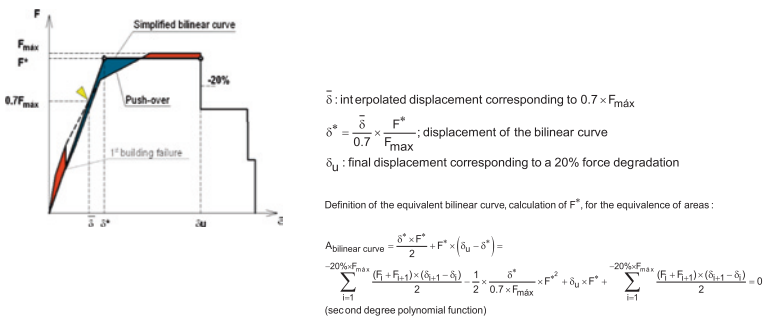


Fig. 25 Construction of the equivalent bilinear curve—case b)

defined in the normal procedure. For this case in Fig. 25 is shown the steps to construct the equivalent elasto-perfectly plastic force–displacement relationship.

- (iv) The construction of the equivalent bilinear capacity curve of an equivalent single degree of freedom is attained by a global transformation factor, Γ_{global} considering the number of floors of each building and the singular transformation factors of each building, to return to a system coordinates of (S_a, S_d) . The transformation factor is given by:

$$\Gamma = \frac{M^*}{\sum_{j=1}^N \frac{m_j^*}{\Gamma_j}} = \frac{\sum_i^N n_{pj} \times m_j^*}{\sum_{i=1}^N \frac{n_{pj}^2 \times m_j^*}{\Gamma_j}}; \Gamma \times m^* = \frac{M^*}{\sum_{j=1}^N \frac{m_j^*}{\Gamma_j}} = \frac{\left(\sum_i^N n_{pj} \times m_j^* \right)}{\sum_{i=1}^N \frac{n_{pj}^2 \times m_j^*}{\Gamma_j}} \quad (30)$$

in which:

$i = 1, \dots, N$ buildings;

m_j^* : $\sum_i m_i \times \Phi_i$; *equivalent mass*;

n_{pj} : number of floors of building;

Γ_j : transformation factor

- (v) Once computed the equivalent bilinear curve, it is possible to evaluate the performance point by using the capacity spectrum method (see Fig. 26). After identifying the final performance point by doing the reverse process the evaluation of the damage state of each building is possible by identifying on each curve the target displacement. In order to access the damage state suffered by

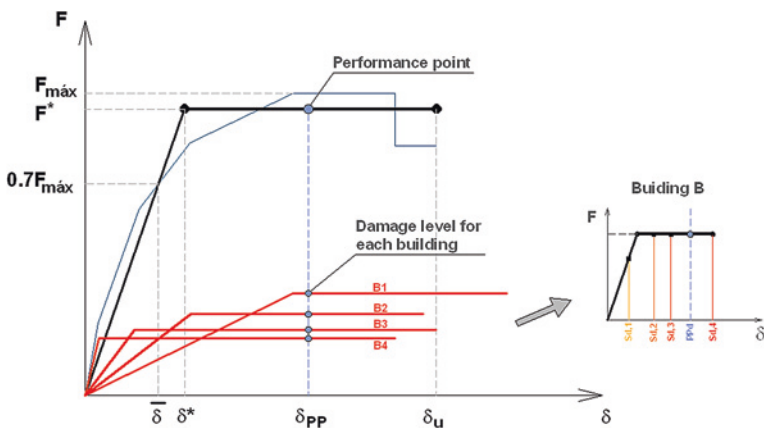


Fig. 26 F- δ curves for each building and performance level identification and limit state definition

Table 6 Thresholds for damage states

Spectral displacement threshold	Damage state
$S_{d,1} = 0.7 \times D_y$	Slight damage
$S_{d,1} = 1.5 \times D_y$	Moderate damage
$S_{d,1} = 0.5 \times (D_y + D_u)$	Severe damage
$S_{d,1} = D_u$	Heavy damage

each building in the aggregate under the defined seismic action, the displacement corresponding to the performance point can then be evaluated. The performance level of each building, by defining the damage threshold states, the values used for the damage state definition have been widely discussed in [51] and are based on expert judgment and for this case are defined as (Table 6):

Once defined the equivalent bilinear curve of the aggregate the performance can be retrieved by applying known procedure for the CSM (see [24]). Then the correspondent displacement is evaluated over the push-over curves for each building, evaluating individually the probabilistic damage distribution for each building and the global response in the direction evaluated. Finally the damage distribution of the aggregate in this direction is evaluated by the average value of the single distribution for each building for only each collapse mode mechanism (soft storey mechanism or uniform collapse) or the global response depending on the direction evaluated, defining in this way a damage range for the building aggregate in this direction, without losing the perception of the damage for each building with the aggregate.

4 Final Remarks

The chapter offers a review and classification of the most commonly adopted procedures for carrying out a seismic vulnerability assessment at territorial scale of large number of historic masonry buildings. By way of exemplification of each of the classes of methods identified, three procedures are presented in greater details. The first one relies on empirical data only and it is an extension of the Vulnerability Index method. By combining this procedure with the vulnerability classes and damage states proposed by EMS'98, it is possible to derive fragility curves, cumulative losses and casualty for building pertaining to diverse vulnerability classes. A simple treatment of the uncertainty is proposed, by using the standard deviation of the Vulnerability Index. This does not account for the uncertainty associated with the hazard.

However, the uncertainties associated with the empirical vulnerability curves and the quality of vulnerability classification data are still issues that must be studied further with respect to post-seismic data collection. For risk mitigation, a reduction in building vulnerability is a priority and therefore the development

of more reliable vulnerability assessment models which combine statistical and mechanical methods should lead to better results.

The second procedure proposed, FaMIVE, represent a robust attempt to meet these requirements. It moves from a survey of the local structural and vulnerability characteristics of the building stock in an historic centre, and uses the collected data within the framework capacity spectrum method and performance base design to derive performance points and fragility curves, for classes of buildings of same typology. Damage thresholds are defined on the basis of observation, numerical analysis and comparison with existing experimental results. The results show that, by considering diverse types of mechanisms, construction details and resilient features, it is possible to tune, capacity curves, first, and then fragility curves, to specific construction typologies and local building characteristics. The aleatoric uncertainty is dealt by considering variability in construction as obtained through the direct survey. The epistemic uncertainty associated with the methodology is accounted for by developing a reliability framework.

Buildings in historic centres are usually built adjacent to each other and their vulnerability is highly affected by the connections to neighbouring buildings. The third procedure shows a first attempt to interpret the overall behaviour of an aggregate by considering in detail the interaction of buildings' facades in plane. This allows deriving capacity curves at the level of the aggregate and captures the global response of the aggregate opening the possibility of defining vulnerability functions at the level of the aggregate based on mechanical behaviour. Out-of plane failures, although classified, have not been considered and this will be a feature extension of the method.

The three procedures illustrated here lend themselves to the use of a GIS platform and database management system to best communicate the information collected about building feature and geometry, the output of seismic vulnerability assessment and the development of damage and other risks scenarios. Such tools, depending on the scale and type of procedure used can be very helpful for the development of strengthening strategies, cost-benefit analyses, civil protection and emergency planning.

References

1. D'ayala, D., Ansal, A.: Non linear push over assessment of heritage buildings in Istanbul to define seismic risk. *Bull. Earthq. Eng.* **10**(1), 285–306 (2012)
2. Benedetti, D., Petrini, V.: Sulla Vulnerabilità Di Edifici in Muratura: Proposta Di Un Metodo Di Valutazione. *L'industria delle Costruzioni* **149**(1), 66–74 (1984)
3. D'ayala, D.: Force and displacement based vulnerability assessment for traditional buildings. *Bull. Earthq. Eng.* **3**(3), 235–265 (2005)
4. D'ayala, D., Spence, R., Oliveira, C.S., Pomonis, A.: Earthquake loss estimation for Europe's historic town centres. *Earthq. Spectra* **13**(4), 773–793 (1997)
5. Mouroux, P., Le Brun, B.: Risk-Ue project: an advanced approach to earthquake risk scenarios with application to different European towns. In: Oliveira, C., Roca, A., Goula, X. (eds.). *Assessing and Managing Earthquake Risk*, vol. 2, pp. 479–508. Springer Netherlands (2006)

6. Calvi, G.M., Pinho, R.: LESSLOSS: A European Integrated Project on Risk Mitigation for Earthquakes and Landslides. University of Pavia, Structural Mechanics Department, Pavia (2004)
7. GNDT-SSN. Scheda di esposizione e vulnerabilità e di rilevamento danni di primo e secondo livello (murata e cemento armato),” *Gruppo Nazionale per la Difesa dai Terremoti, Roma* (1994)
8. Grünthal, G.: European Macroseismic Scale 1998 (EMS-98), European Seismological Commission, Subcommittee on Engineering Seismology, Working Group Macroseismic Scales,” *Cahiers du Centre Européen de Géodynamique et de Séismologie*, vol. 15, (1998)
9. Whitman, R.V., Reed, J.W., Hong, S.T.: Earthquake damage probability matrices. In: *Proceedings of the 5th World Conference on Earthquake Engineering, Rome*, vol. 2, pp. 2531–2540, (1973)
10. Calvi, G.M.: A displacement-based approach for vulnerability evaluation of classes of buildings. *J. Earthq. Eng.* **3**(03), 411–438 (1999)
11. Speranza, E.: *An Integrated Method for the Assessment of the Seismic Vulnerability of Historic Buildings*. University of Bath (2003)
12. ATC-40. Seismic evaluation and retrofit of concrete buildings. Technical report, ATC-40. Applied Technology Council, Redwood City, California (1996)
13. FEMA 273. NEHRP Guidelines for the Seismic Rehabilitation of Buildings: Second Ballot Version. The Council (Federal Emergency Management Agency), Washington DC (1997)
14. Fajfar, P.: Capacity spectrum method based on inelastic demand spectra. *Earthq. Eng. Struct. Dynam.* **28**(9), 979–994 (1999)
15. ATC-21. Rapid Visual Screening of Buildings for Potential Seismic Hazards: A Handbook. Redwood City, California (1988)
16. ATC-13. Earthquake damage estimation data for California. Report ATC-13. Applied Technology Council, Redwood City, California (1985)
17. HAZUS. Earthquake loss estimation methodology—technical and user manual. Federal Emergency Management Agency, Washington, D.C. (1999)
18. FEMA 178. NEHRP Handbook for the Seismic Evaluation of Existing Buildings. The Council (Federal Emergency Management Agency), Washington, DC (1992)
19. Lagomarsino, S., Giovinazzi, S.: Macroseismic and mechanical models for the vulnerability and damage assessment of current buildings. *Bull. Earthq. Eng.* **4**(4), 415–443 (2006)
20. Santos, C., Ferreira, T.M., Vicente, R., Mendes da Silva, J.A.R.: Building typologies identification to support risk mitigation at the urban scale—case study of the old city centre of Seixal, Portugal. *J. Cult. Heritage* (2012)
21. Vicente, R., Parodi, S., Lagomarsino, S., Varum, H., Mendes da Silva, J.A.R.: Seismic vulnerability and risk assessment: case study of the historic city centre of Coimbra, Portugal. *Bull. Earthq. Eng.* **9**(4), 1067–1096 (2011)
22. Ferreira, T.M., Vicente, R., Mendes da Silva, J.A.R., Varum, H., Costa, A.: Seismic vulnerability assessment of historical urban centres: case study of the old city centre in Seixal, Portugal. *Bull. Earthq. Eng.* 1–21 (LA—English) (2013)
23. Ferreira, T., Vicente, R., Varum, H., Mendes da Silva, J.A.R., Costa, A.: Vulnerability assessment of urban building stock: a hierarchic approach. In: *International Disaster and Risk Conference IDRC*, pp. 245–248 (2012)
24. Vicente, R.: *Estratégias e metodologias para intervenções de reabilitação urbana. Avaliação da vulnerabilidade e do risco sísmico do edificado da Baixa de Coimbra*. PhD Thesis. Universidade de Aveiro, Portugal. (in Portuguese), (2008)
25. Giovinazzi, S.: *The vulnerability assessment and the damage scenario in seismic risk analysis*. Technical University Carolo-Wilhelmina at Braunschweig, Braunschweig, Germany and University of Florence, Florence (2005)
26. Bernardini, A., Giovinazzi, S., Lagomarsino, S., Parodi, S.: Vulnerabilità e previsione di danno a scala territoriale secondo una metodologia macrosismica coerente con la scala EMS-98. In: *ANIDIS, XII Convegno Nazionale l’ingegneria sismica in Italia* (2007)

27. Sandi, H., Floricel, I.: Analysis of seismic risk affecting the existing building stock. In: Proceedings of the 10th European Conference on Earthquake Engineering, vol. 3, pp. 1105–1110 (1995)
28. Bramerini, F., Di Pasquale, G., Orsini, A., Pugliese, A., Romeo, R., Sabetta, F.: Rischio sismico del territorio italiano. Proposta per una metodologia e risultati preliminari. Servizio Sismico Nazionale, Rapporto Tecnico, SSN/RT/95/01, Roma, (1995)
29. Coburn, A., Spence, R., Comerio, M.: Earthquake protection. *Earthq. Spectra* **19**, 731 (2003)
30. Tiedemann, H.: Casualties as a function of building quality and earthquake intensity. In: Proceedings of the International Workshop on Earthquake Injury Epidemiology for Mitigation and Response, pp. 10–12 (1989)
31. Dolce, M., Kappos, A., Masi, A., Penelis, G., Vona, M.: Vulnerability assessment and earthquake damage scenarios of the building stock of Potenza (Southern Italy) using Italian and Greek methodologies. *Eng. Struct.* **28**(3), 357–371 (2006)
32. Di Pasquale, G., Goretta, A.: Economic and functional vulnerability of residential buildings stricken by Italian recent seismic events. In: Proceedings of the 10th Italian National Conference on Earthquake Engineering (2001)
33. D’Ayala, D., Speranza, E.: Definition of collapse mechanisms and seismic vulnerability of historic masonry buildings. *Earthq. Spectra* **19**(3), 479–509 (2003)
34. CEN. Eurocode 8: design of structures for earthquake resistance. Part 3: General Rules, Seismic Actions and Rules for Buildings, prEN 1998-1. CEN, Brussels (2005)
35. D’Ayala, D., Kansal, A.: Analysis of the seismic vulnerability of the architectural Heritage in Buhj, Gujarat, India. In: Proceedings of IV International Seminar on Structural Analysis of Historical Constructions, pp. 1069–1078 (2004)
36. D’Ayala, D., Paganoni, S.: Assessment and analysis of damage in L’Aquila historic city centre after 6th April 2009. *Bull. Earthq. Eng.* **9**(1), 81–104 (2011)
37. D’Ayala, D., Shi, Y.: Modeling Masonry Historic Buildings by Multi-Body Dynamics. *Int. J. Architect. Heritage* **5**(4–5), 483–512 (2011)
38. Bosiljkov, V., Kržan, M., D’Ayala, D.: Vulnerability study of Urban and rural heritage masonry in Slovenia through the assessment of local and global seismic response of buildings. In: Proceedings of the 15th World Conference on Earthquake Engineering (2012)
39. EERI. Final Technical Report- Providing building vulnerability data and analytical fragility functions for PAGER (2012)
40. D’Ayala, D., Kishali, E.: Analytically derived fragility curves for unreinforced masonry buildings in urban contexts. (2012)
41. Paquette, J., Bruneau, M.: Pseudo-dynamic testing of unreinforced masonry building with flexible diaphragm and comparison with existing procedures. *Constr. Build. Mater.* **20**(4), 220–228 (2006)
42. Magenes, G., Penna, A., Rota, M., Galasco, A., Senaldi, I.: Shaking table test of a full scale stone masonry building with stiffened floor and roof diaphragms. In: Proceedings of the 15th World Conference on Earthquake Engineering (2012)
43. Meisl, C., Elwood, K., Ventura, C.: Shake table tests on the out-of-plane response of unreinforced masonry walls this article is one of a selection of papers published in this special Issue on Masonry. *Can. J. Civ. Eng.* **34**(11), 1381–1392 (2007)
44. Griffith, M.C., Lam, N.T.K., Wilson, J.L., Doherty, K.: Experimental investigation of unreinforced brick masonry walls in flexure. *J. Struct. Eng. ASCE* **130**(3), 423–432 (2004)
45. D’Ayala, D., Shi, Y., Stammers, C.W.: Dynamic multibody behaviour of Historic masonry building models. In: Proceedings of the VI International Conference on Structural Analysis of Historic Construction, SAHC08, vol. I, pp. 489–496 (2008)
46. Al Shawa, O., De Felice, G., Mauro, A., Sorrentino, L.: Out-of-plane seismic behaviour of rocking masonry walls. *Earthq. Eng. Struct. Dynam.* **41**(5), 949–968 (2012)
47. Tomažević, M.: Damage as a measure for earthquake-resistant design of masonry structures: slovenian experience this article is one of a selection of papers published in this special Issue on masonry. *Can. J. Civ. Eng.* **34**(11), 1403–1412 (2007)

48. Jaiswal, K., Wald, D., D'Ayala, D.: Developing empirical collapse fragility functions for global building types. *Earthq. Spectra* **27**(3), 775–795 (2011)
49. Freeman, S.A.: Review of the development of the capacity spectrum method. *ISSET J. Earthq. Technol.* **41**(1), 1–13 (2004)
50. Griffith, M.C., Vaculik, J., Lam, N.T.K., Wilson, J., Lumantarna, E.: Cyclic testing of unreinforced masonry walls in two-way bending. *Earthq. Eng. Struct. Dynam.* **36**(6), 801–821 (2007)
51. Kappos, A.J., Panagopoulos, G., Penelis, G.G.: Development of a seismic damage and loss scenario for contemporary and historical buildings in Thessaloniki, Greece. *Soil Dynam. Earthq. Eng.* **28**(10–11), 836–850 (2008)
52. Giuffrè, A.: Mechanics of historical masonry and strengthening criteria. In: *Proceedings of the XV Regional Seminar on Earthquake Engineering*, pp. 60–122 (1989)
53. Pagnini, L.C., Vicente, R., Lagomarsino, S., Varum, H.: A mechanical model for the seismic vulnerability assessment of old masonry buildings. *Earthq. Struct.* **2**(1), 25–42 (2011)